A NONEQUILIBRIUM THERMODYNAMIC MODEL OF ION TRANSPORT

IN A THREE-COMPARTMENT SYSTEM

By

Heinz George Hausch

BAE, Rensselaer Polytechnic Institute, 1963

Thesis

submitted in partial fulfillment of the requirements for the

)egree of Doctor of Philosophy in the Department of Physiology

at the Medical College of Virginia, Health Sciences Center,

Virginia Commonwealth University

Richmond, Virginia

June, 1970

This thesis by Heinz George Hausch is accepted in its present form as satisfying the thesis requirement for the degree of Doctor of Philosophy

Date: Approved:

April 23, 1970   *Robert E. Thurber*
                                   Advisor, Chairman of Graduate Committee

May 11, 1970   *Leslie E. Edwards*

May 11, 1970   *C. M. Parke*

May 11, 1970   *Samuel Katzoff*

May 11, 1970   *L. B. Abbott*

Approved: *Daniel J. Watts*
                  Dean of the School of Graduate Studies

iii

CURRICULUM VITAE

The author ████████████. ██ ████, ██████, ████. He
received his early education at the Humboldtschule in Hanover, Germany.
He came to the United States in 1951, and continued his education in
the Lower Moreland Township Public School System in Huntingdon Valley,
Pennsylvania, where he graduated from high school in June of 1959. He
entered the Rensselaer Polytechnic Institute as an undergraduate in
the fall of that year, and spent the next four years in the pursuit of
the Bachelor's degree in Aeronautical Engineering.

Upon receiving the B.A.E. degree in June of 1963 from R.P.I., the
author became employed by the Langley Research Center of the National
Aeronautics and Space Administration in Hampton, Virginia. There he
became involved primarily in work on life support systems for extended
manned space flights.

While at the Langley Research Center, he continued his education
with undergraduate work in chemistry and biology at the College of
William and Mary, and graduate work in mathematics and statistics at
the University of Virginia and the Virginia Polytechnic Institute. He
enrolled as a graduate student in the Department of Physiology at the
Medical College of Virginia in the summer of 1965.

During the fall of 1965, while at the Medical College of Virginia,
he married the former Jane Tyler Tallman of Richmond, Virginia.

He is currently employed by the Langley Research Center as an
Aero-Space Technologist.

iv

ACKNOWLEDGMENTS

The author wishes to thank his advisor, Professor R. E. Thurber, for his suggestions, constructive criticisms, and overall encouragement during the course of his study.

The author would also like to express his gratitude to his section head at the Langley Research Center, R. A. Bruce, for the many helpful suggestions during the performance of this research.

The computer programing of the analytical model was performed by Mrs. W. W. Smith at the Langley Research Center. The author would like to offer a special thanks to her.

Finally, the author would like to express his gratitude to the Langley Research Center for making the course of study and research work possible.

v

TABLE OF CONTENTS

Page

LIST OF FIGURES

Page

LIST OF TABLES

SUMMARY

A physical analog of steady-state sodium and potassium transport
in a two-membrane, three-compartment system was studied utilizing the
principles of nonequilibrium thermodynamics. This physical system is
analogous to physiological systems where one compartment consisting of
a cell monolayer separates two other compartments, such as the inter-
stitial fluid and the renal tubule lumen in the kidney. The membranes
in the model system serve only to localize the chemical potential
gradients between compartments. The phenomenological equations relating
the flows through the membranes to the chemical potential gradients
were developed from the equation for energy dissipation within each
membrane. The flows defined both the nonsteady-state rates of change
of concentrations within each compartment and the steady-state transport
across each membrane.

Ion transport due to chemical convection was studied by adding
water to the "cell" compartment and removing it from the "interstitial"
compartment. The "lumen" compartment was left as a strictly passive
compartment. The Na^+, K^+, and Cl^- concentrations were measured
periodically until a steady-state was reached.

In further experiments the concentrations of components in the
"lumen" compartment were held constant by a constant flow of
$NaCl-KCl-H_2O$ solution through the compartment. The constant flow of
water into the "cell" compartment distributed itself among both the
"lumen" and "interstitial" compartments according to the mechanical

filtration properties of each membrane. In initial experiments, the flows were unidirectional into the "interstitial" compartment. In later experiments the flow was distributed to both the "interstitial" and "lumen" compartments. After the system had reached a steady-state, the concentrations of components, the flows of solution in and out of the "lumen" compartment, and the flow of water into the "cell" compartment were measured. The magnitudes and directions of the steady-state transport of components were determined.

The nonsteady-state experiments demonstrated a transient transport of Na^+, K^+, and Cl^- ions from the "lumen" compartment to the "interstitial" compartment against a concentration gradient. At low solvent fluxes the ion transport occurs with the concentration gradient. At intermediate solvent fluxes, K^+ and Na^+ are transported in opposite directions; K^+ is transported down a concentration gradient while Na^+ is transported against an equal or larger gradient.

Steady-state transport of Na^+ and K^+ from the "lumen" compartment to the "interstitial" compartment may be maintained by a solvent flux in the direction of transport. The magnitude of this transport is greatest when the concentrations of components in the two compartments are equal, and decreases as the concentration ratio of components in the "intestitial" compartment to those in the "lumen" increases. For the combinations of solvent fluxes and component concentrations investigated, the transport of K^+ was usually greater than the transport of Na^+.

INTRODUCTION

An important problem in the field of biology concerns the ability
of living cells to maintain stationary nonequilibrium distributions of
molecular components across their membranes and the associated ability
of a layer of such cells to maintain a constant flow of molecular
components from one side to the other against concentration gradients
of the components.

Classical approaches dealing with this phenomenon are summarized
in general physiology texts (2, 4, 5, 11, 12). The system generally
considered is one of two compartments, cellular and interstitial,
separated by a cell membrane. Transport is considered to be at
steady-state. If the component is such that it is neither produced
nor consumed within the cell, the net transport is zero. If the
material transported is produced or consumed at a certain rate, then
the transport must proceed at a rate equal to production or consumption.
The effect of the transport is to maintain a constant concentration of
materials within the cell, a factor vital to the viability of the cell.

A more complicated situation exists when the cell compartment
separates two different extracellular compartments, such as occurs in
the kidney tubule, intestinal mucosa, and capillary endothelium. In
this case, a steady-state transport of a material, which is neither
consumed nor produced within the cell, can exist across the cell
membrane without altering the concentration of the material within the
cell. The material enters the cell at a certain rate from one

compartment and leaves the cell at the same rate into the other compartment. Such a system maintains constant concentrations of components within an organ and within the organism as a whole.

Classical descriptions of biological transport generally categorize transport as passive or active. Passive transport is defined as that which occurs without the utilization of metabolic energy produced at the local site of transport. It is a process spontaneously driven by an electrochemical gradient negative in the direction of transport and with a simultaneous decrease in the free energy of the system.

Active transport is defined as transport phenomena that require utilization of metabolic energy at the site of transfer. In this case, material may be transported against an electrochemical gradient, and the change in free energy in the local system becomes positive. By this mechanism a living cell may maintain concentration differences in the face of passive gradients, or, in the case of a tissue layer, this mechanism provides a means for sustaining a constant, steady-state transport of material against an electrochemical potential gradient. The above definitions hold true when the mechanism observed is purely passive or purely active. However, in most situations these mechanisms occur simultaneously. Various classical criteria have been developed for determining whether active transport is taking place. The most noted are the Nernst equation and the Ussing criterion.

The Nernst equation (2) for zero net ion flux is generally written as

1) $$E_2 - E_1 = \frac{RT}{zF} \, \ln(C_1/C_2)$$

where E denotes electrical potential, C denotes ion concentration, F is the Faraday constant, R is the universal gas constant, T is absolute temperature, and z denotes the charge of the ion. The numbers 1 and 2 denote the intra and extracellular compartments. When the transport phenomenon is strictly passive, a concentration gradient is balanced by an electrical gradient, and the Nernst equation is followed. When the Nernst equation is not followed, the concentration and electrical gradients are out of balance, resulting in a concentration gradient component unaccounted for by the passive forces defined in the Nernst equation. This requires the addition of an active transport component.

The Ussing criterion (2, 39) relates the ratio of the unidirection fluxes of a component, i.e., fluxes of the same material in opposing directions, to the concentration ratio and electrical potential difference across the membrane:

2) $$\left| \frac{M_{2,1}}{M_{1,2}} \right| = \frac{C_2}{C_1} \, e^{\frac{zF}{RT}(E_2 - E_1)}$$

$M_{2,1}$ is the flux of the material from side 2 to side 1, while $M_{1,2}$ is the flux from side 1 to side 2. C_2 and C_1 are the concentrations on sides 2 and sides 1 of the membrane. $E_2 - E_1$ is the electrical potential difference. If the ratio of unidirectional fluxes relates to the concentrations and electrical potentials as defined by the Ussing equation, passive mechanisms are sufficient to account for the transport phenomena. If, however, the Ussing equation is not followed, active mechanisms are hypothesized to account for the unbalance. The unidirectional fluxes may be experimentally determined by utilizing a radioactive isotope of the material on one side of the membrane.

Since it is difficult to investigate the molecular processes occurring on the membrane surface and within the membrane, the specific mechanisms of active transport are not known. However, several hypotheses have been proposed. The two hypotheses that are currently most popular relate active transport to carrier-mediated movement and directional binding sites within the membrane (2, 20, 41). In the first hypothesis, the ion to be transported is bound to a carrier molecule on one side of the membrane, diffuses through the membrane as a complex, and is dissociated from the carrier at the other side. The energy for the dissociation is derived from the breakdown of a high energy compound. In the case of sodium transport out of a cell and potassium transport into a cell, the carrier molecule is thought to be sodium-potassium-activated adenosine triphosphatase and the energy for dissociation is provided by the breakdown of ATP to the lower energy compound ADP.

The directional binding site hypothesis contends that the membrane pore is lined with binding sites with specificity for the ion transported and with directional characteristics such that the sites bind the ion more strongly in one direction than in the opposing direction. Utilizing energy from the breakdown of high energy compounds, the bond configuration of the binding site is thought to change and release the bound ion.

One problem of the classical approach to ion transport is that it treats each component as a separate entity, thus creating a multitude of one-component systems. This requires that the free energy for each process decrease in order for the transport of that component to occur spontaneously and therefore be of a passive nature. If a change in free energy is positive, the transport needs an active mechanism in order to occur. What is neglected is the irreversible frictional interaction or coupling between component processes. If this coupling factor is included in a multicomponent treatment, the only requirement for transport to occur passively is that the total change in free energy for all components be negative. If the changes in free energy for the transport of all but one component are positive, the total change in free energy for the entire process may still be negative, and the entire process is essentially passive.

Biological ion transport is a nonequilibrium phenomenon that cannot be explained in classical equilibrium terminology. A better approach to this problem may be found in the realm of nonequilibrium thermodynamics.

The groundwork for the theoretical approach to the thermodynamics of irreversible processes or nonequilibrium thermodynamics was laid by Onsager (28) in 1931, for which he received the Nobel Prize in Chemistry in 1968. Onsager employed Lord Rayleigh's original treatise on the theory of sound which presented a set of equations expressing the linear dependence of mechanical flows on mechanical forces. Onsager extended these equations to include thermodynamic flows and forces. The resulting equations are known as phenomenological equations:

$$J_1 = L_{11}X_1 + L_{12}X_2 \cdots$$
$$J_2 = L_{21}X_2 + L_{22}X_2 \cdots$$

3)
$$\cdot$$
$$\cdot$$
$$\cdot$$

$$J_n = L_{n1}X_1 + L_{n2}X_2 \cdots$$

or

4)
$$J_i = \sum_{k=1}^{n} L_{ik}X_k \qquad (i = 1, 2, \dots n)$$

J_i are specific flows or processes and X_k are forces. L_{ii} are the "straight" coefficients relating the flows to their conjugate forces. Examples of the relationship of flows to conjugate forces include the flow of heat as a result of a temperature gradient, the flow of electric current as a result of an electrical potential gradient, and the diffusion of an ion as a result of its own chemical potential

gradient (17). L_{ik} (k ≠ i) are the "cross" coefficients. These relate flows to nonconjugated forces. Examples of this relationship include flow of current as a result of a temperature gradient and the flow of volume as a result of an electrical potential gradient (17). The cross coefficients also relate the flow of an ion to the nonconjugated force consisting of a pressure gradient or a chemical potential gradient of a different ion species. The phenomenological · equations in the application to multicomponent systems become an extension of Fick's first law.

The thermodynamics of irreversible processes based on Onsager's original work has since been developed more fully by Meixner, de Groot, Casimir, and Prigogine, and summarized in texts by Denbigh (6), de Groot (14), de Groot and Mazur (15), Fitts (9), Prigogine (31), Van Rysselberghe (40), and Haase (16). Katchalsky and Curran (19) combined the various approaches to make the theory more amenable to biological problems.

The concept basic to the theory of nonequilibrium thermodynamics is that of entropy. According to the second law of thermodynamics, the change in entropy for a quasi-static, reversible process is equal to the change in heat divided by the absolute temperature:

5) $$dS = \frac{dQ}{T}$$

This relationship does not hold for irreversible processes where

6)
$$dS > \frac{dQ}{T}$$

For example, in a reversible adiabatic process where the heat exchanged, dQ, is zero, the entropy remains constant $(dS = 0)$. However, in an irreversible. adiabatic process, the entropy of the system increases. This makes the entropy ideal for a qualitative differentiation between reversible and irreversible processes. Equation 6 does not give any information other than the direction in which a process will go. The approach to quantitative formulation of the nonequilibrium thermodynamics is to replace the inequality in equation 6 with an equality in order to be able to precisely specify what the entropy change actually is. The assumption is made that the entropy of a system at any point of the irreversible process is only a function of the parameters that totally characterize the system at that point regardless of how that point was reached. If this is so, then the entropy at a specific point in the irreversible process would be equal to the entropy of the system if the nonequilibrium distribution of internal parameters were maintained at equilibrium by an external reversible process. Since the entropy of the resulting equilibrium system and of the external reversible processes can now be defined by equilibrium thermodynamics, the total entropy of the corresponding nonequilibrium system may be determined.

The next important step in the development of nonequilibrium thermodynamic theory is the postulation that the total entropy change in an irreversible process is equal to the sum of the entropy exchanged

by the system with its surroundings, or external entropy, and the entropy created within the system, or internal entropy:

$$7) \qquad dS = dS_{ext} + dS_{int}$$

The internal entropy production is greater than zero for all irreversible processes and equal to zero for all reversible processes. Now, the internal entropy, dS_{int}, is related to the local entropy production, σ, as follows:

$$8) \qquad \frac{dS_{int}}{dt} = \int_V \sigma dV$$

Thus, the local entropy production is the entropy produced in a unit volume per unit time. The local entropy production is a highly sophisticated concept that relates all flows and their conjugate forces:

$$9) \qquad \sigma = \sum_{i=1}^{n} J_i X_i$$

Derived from and very often used instead of the local entropy production is the dissipation function, ϕ:

$$10) \qquad \phi = T\sigma = T \sum_{i=1}^{n} J_i X_i$$

The dissipation function always relates the flows and forces such that it is equal to the rate of conversion of free energy into thermal energy.

, Both the local entropy production and the dissipation function
define a set of phenomenological equations:

11)
$$J_i = \sum_{k=1} L_{ik}X_k$$

L_{ik}, the phenomenological coefficients, are generalized mobilities or
conductances. The phenomenological equations may also be written in
terms of generalized frictions or resistances, R_{ik}.

12)
$$X_i = \sum_{k=1}^{n} R_{ik}J_k$$

Onsager (28) in his original work demonstrated that if the flows
and forces are so related as to define the local entropy production,
σ, or the dissipation function, ϕ, then the following relationship
for the cross-coefficients hold:

13)
$$L_{ik} = L_{ki} \qquad (i \neq k)$$
$$R_{ik} = R_{ki} \qquad (i \neq k)$$

These relationships are known as the Onsager law of reciprocal
relations. This law is very important in terms of practical applica-
tion of the phenomenological equations since it reduces significantly .
the number of unknown coefficients. The law has been proven experi-
mentally for multicomponent diffusion by Dunlop and Gosting (7).

Based on his earlier work, Onsager (29) applied nonequilibrium thermodynamics to the problem of diffusion. First, he developed a generalization of Fick's law for multicomponent systems:

$$14) \qquad J_i = -\sum_{k=1}^{n} D_{ik} \nabla C_k$$

J_i is the diffusion flow of component i, D_{ik} is the diffusion coefficient relating the ith flow to the kth concentration gradient, ∇C_k. Then, utilizing the dissipation function for multicomponent diffusion, Onsager related the diffusion flows, J_k, to the thermodynamic properties of the solution:

$$15) \qquad - \nabla \mu_i = \sum_{k=1}^{\leftrightarrow} R_{ik} J_k$$

where $\nabla \mu_i$ is the chemical potential gradient of component i, and R_{ik} is the resistance coefficient relating the ith force to the kth flow.

Hearon (18) applied Onsager's theoretical work to the problem of cellular diffusion. He related the distributions of metabolic solute and inert solutes, $\nabla^2 C_k^{int}$ (where C_k^{int} is the concentration of the component inside the cell) to the rates of production and/or consumption of the various metabolic solutes, q_i, within the cell:

$$16) \qquad \nabla^2 C_k^{int} = -\sum_{i} q_i R_{ki}$$

R_{ki} is the resistance coefficient relating the ith flow, q_i, to the kth force. Solutions to equation 16 demonstrate that metabolic solutes may flow continually against their concentration gradients and inert solutes may establish nonequilibrium, stationary concentration gradient across the membrane. As a consequence of this frictional coupling, or coupling with diffusion, the rates of production or consumption of one metabolic solute may influence the metabolism of another metabolically unrelated substrate. Furthermore, a change in the metabolic rates may result in the flow of metabolically inert solute from a region of low concentration to a region of high concentration.

Stavermann (37) applied nonequilibrium thermodynamic theory directly to membrane processes. Specifically, he related molecular transport, $\dot{n}_i$, across a membrane to three forces: electrical potential difference across the membrane, ΔE, pressure difference, ΔP, and chemical potential difference, $\Delta \mu_k$:

$$17) \qquad \dot{n}_i = \sum_k L_{ik}(z_k \Delta E + \overline{V}_k \Delta P + \Delta \mu_k)$$

z_k is the charge and $\overline{V}_k$ is the partial molar volume of the kth ion. He also related the phenomenological coefficients, L_{ik}, which cannot be measured directly, to experimentally measurable quantities.

Kedem and Katchalsky (21) modified and extended Staverman's work to the permeability of biological membranes. They demonstrated the unacceptability of the conventional equations for osmotic and pressure

induced flows across the membrane. The conventional equations involve two coefficients: the permeability coefficient of the solute and the permeability coefficient of the solvent. However, in order to totally describe the membrane transport process, three coefficients are required: the diffusion coefficient of the solute relative to the solvent, a coefficient related to the friction between membrane and solvent, and a coefficient related to the friction between solute and membrane. The equations for volume flow, J_V, and diffusion flow, J_D, in terms of these three coefficients are:

$$J_V = L_P \Delta P + L_{PD} RT \Delta C_s$$

18)

$$J_D = L_{DP} \Delta P + L_D RT \Delta C_s$$

L_P is the mechanical filtration coefficient related to the friction between membrane and solvent, L_D is the diffusion coefficient related to the friction between solvent and solute, and $L_{DP}(= L_{PD})$ is the coefficient related to the friction between solute and membrane. Equations 18 not only describe bulk flow and diffusion flow, but as a result of the cross-coupling coefficients, L_{PD}, describe osmosis (the flow of solvent resulting from a concentration differential) and ultrafiltration (the flow of solute resulting from a pressure differential). Kedem and Katchalsky developed mathematical criteria for quantifying the selectivity of membranes, and derived equations analogous to equations 18, for a multicomponent system with

a single permeable solute as a·function of reflection coefficients, σ, and solute permeabilities, ω.

Manning (24), to characterize the membrane more precisely, extended Kedem and Katchalsky's equations by assuming that the diffusion and bulk flow occurred through specific potential energy profiles within an idealized membrane. He derived expressions for reflection coefficients and solute permeabilities as functions of the potential energy profiles.

Spiegler (36), Nims (25), and Kedem and Katchalsky (22) have developed mechanical approaches to describe irreversible ion transport and membrane processes. The approach is based on the law of friction which relates the frictional force between two objects linearly to the relative velocity of their motion. A multicomponent system is characterized by the relative velocities and the friction coefficients between the various components and between the components and the membrane. The resulting equations demonstrate the following relation-ships between the mechanical friction coefficients, f_{ki}, and the thermodynamic coefficients, R_{ki}, and D_{ki}:

19)
$$R_{ki} = \frac{f_{ki}\triangle x}{C_i A}$$

$$D_{ki} = \frac{RT}{f_{ki}}$$

$\triangle x$ is the thickness and A is the area of the membrane, R is the universal gas constant, and T is the absolute temperature.

Nims (25) showed that the nonequilibrium stationary distribution of Na^+, K^+, and Cl^- ions produced by a constant water flux across a porous membrane is defined by the diffusion coefficients of the ions relative to water:

20) $$\frac{\ln \frac{c^{\beta}_{Na^+}+c^{\beta}_{Cl^-}-\gamma^{\beta}_{Na^+}+\gamma^{\beta}_{Cl^-}}{c^{\alpha}_{Na^+}+c^{\alpha}_{Cl^-}-\gamma^{\alpha}_{Na^+}+\gamma^{\alpha}_{Cl^-}}}{\ln \frac{c^{\beta}_{K^+}+c^{\beta}_{Cl^-}-\gamma^{\beta}_{K^+}+\gamma^{\beta}_{Cl^-}}{c^{\alpha}_{K^+}+c^{\alpha}_{Cl^-}-\gamma^{\alpha}_{K^+}+\gamma^{\alpha}_{Cl^-}}} = \frac{D_{(KCl)w}}{D_{(NaCl)w}} \approx 1.2$$

α and β are the two compartments on either side of the membrane, and γ is the activity coefficient of the specific ion in the respective compartment.

The premise that a stationary nonequilibrium distribution of ions across the membrane may be maintained by a flow of other components has been tested by a number of experiments. Nims and Thurber (26) used a two compartment plastic apparatus with a Millipore filter membrane separating the compartments to determine the distribution of Li^+, Na^+, K^+, and Cl^- ions across the membrane. A constant flow of water was added to one compartment, and removed by evaporation from the second compartment. After the system had reached a stationary state, Na^+, K^+, and Li^+ concentrations were determined. The distributions according to equation 20 were calculated at various flows of water. Experimental values compared well with the theoretical value of 1.2.

Salminen (33) devised an experiment to test theoretical data developed by Ekman, Rastas, and Salminen (8). The theoretical system,

based on nonequilibrium thermodynamics, involved two compartments
connected by a capillary pore. Stationary nonequilibrium ion distri-
butions within the capillary were calculated as a function of a flow
of hydrochloric acid and water. The experimental apparatus was very
similar to that of Nims and Thurber (26). A constant flow of water
and hydrochloric acid was maintained across the membrane. Hydrochloric
acid, added to one compartment, reacted in the other compartment with
sodium hydroxide. The experimental and theoretical results demonstrated
that Na^+ and K^+ may be transported in opposite directions across a
membrane against their concentration gradients by utilizing constant
flows of acid and water.

In experiments similar to those of Nims and Thurber (26), Rapoport
(32) demonstrated nonequilibrium stationary distribution of K^+, Li^+,
and Cl^- across a porous membrane using a constant flow of water.

Nims and Butera (27) demonstrated a nonequilibrium stationary
distribution of ions across a membrane resulting from a constant flux
of urea, ammonium, and carbon dioxide. Urea was added at a constant
rate to one compartment and hydrolyzed by urease in the second
compartment. The ions moved both against their concentration and
electrochemical gradients.

Thurber and Thompson (38) experimentally tested the prediction
based on nonequilibrium thermodynamics that the stationary ion
distributions across a membrane are exponentially related to the steady-
state metabolic flows across the membrane. The investigators utilized

human erythrocytes under anaerobic conditions. In this case the total
flow of metabolites was approximated by the lactic acid production, $\dot{n}_L$,
and the ion distribution was expressed as

$$\ell n \; \frac{Na_p K_c}{Na_c K_p} \; = \; \frac{M\dot{n}_L}{T}$$

where p and c refer to the plasma and cell compartments, M is a
summation of membrane parameters and frictional coefficients, and T
is the absolute temperature. The erythrocytes were incubated at
various temperatures. Stationary state lactic acid production and
cellular and plasma concentrations of Na^+ and K^+ were determined. The
experimental data correlated with equation 21 within experimental
error, and the investigators concluded that the equation was a valid
description of nonequilibrium ion distribution in the human erythrocyte.

The thermodynamic and mechanical treatment of transport across
membranes as reviewed above generally describe macroscopic phenomena.
In a biological membrane, however, the pores and associated transport
phenomena are on the microscopic level, i.e., of the order of magnitude
of the molecular components. Thurber and Thompson's work (38) is
particularly significant in that it demonstrates the validity of the
macroscopic equations as applied to a biological system.

The objective of my investigation was to extend the above described
work to a two-membrane, three-compartment system, which is open to all
components, and to determine whether a flow of one of the components
can maintain a nonequilibrium stationary distribution of ions, and

whether such a flow can sustain steady-state transport of ions against
their concentration gradients.

The two-membrane, three-compartment system is a simple model of
cell layers, such as exist in the kidney tubule, the intestinal mucosa,
and the capillary endothelium. The cell layer, compartment β, separate:
two other compartments: the lumen, compartment α; and the interstitial
space, compartment γ. There are two membranes separating the compart-
ments. Metabolic substrates are consumed or produced within the cell
compartment, producing material flows across the membranes. These
flows may be different across each membrane if the physical properties
of the membranes are different or if the chemical potential of the
substrates are different in the external compartments. The flows are
a source of free energy, and may, by frictional cross-coupling, produce
flows of metabolically inert components.

This model despite the simplifying assumptions, can throw light
on the question of how a cell layer can maintain nonequilibrium
distributions of ions to which it is permeable, and how it can sustain
steady-state transport of these ions against their concentration
gradients.

A mathematical model of this system was developed from non-
equilibrium thermodynamic theory for isothermal conditions and
continuous phases. It was assumed that no gradients existed within
the compartments. Components consisted of NaCl and KCl in aqueous
solution. The "metabolic" production of water within the cellular
compartment, β, was the only metabolic substrate or product flow

considered in this model. The water flow distributed itself between the external compartments, α and γ, according to the pressure differentials across the membranes and the mechanical filtration properties of the membranes. The membranes localized the chemical potential or concentration gradients between the solutions in the compartments. The membranes were assumed not to differentiate between ion components. Consequently, no flow of current through and no separation of charge across the membrane were considered. The membranes were assumed to be homogeneous at every elemental thickness and the effective pore area was assumed constant throughout the membrane. Although these assumptions are severe, they portray a limiting case, and any observed phenomena may differ from the real case only in magnitude.

Initially, the system, as in Figure 1 was studied under conditions where the system is open only to a unidirectional flow of water from the "cellular" compartment, β, to the "interstitial" compartment, γ. The concentrations of ions in γ were held constant by virtue of the relatively large size of that compartment. The intent was to observe the direction of transient ion transport as a function of the water flow. In the limiting case, where time approaches infinity, this system becomes a stationary two-compartment system of the first order, and ion distributions may be calculated according to Nims (25).

Next, the system shown in Figure 2 was studied under conditions where the system was open to NaCl and KCl, as well as to a unidirectional flow of water from the "cellular" compartment, β, to the "interstitial"
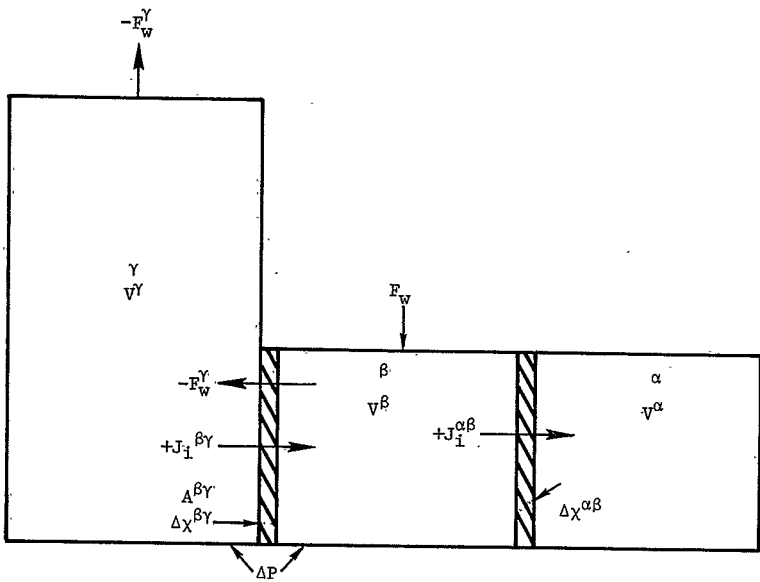
Figure 1.- Nonsteady-State System
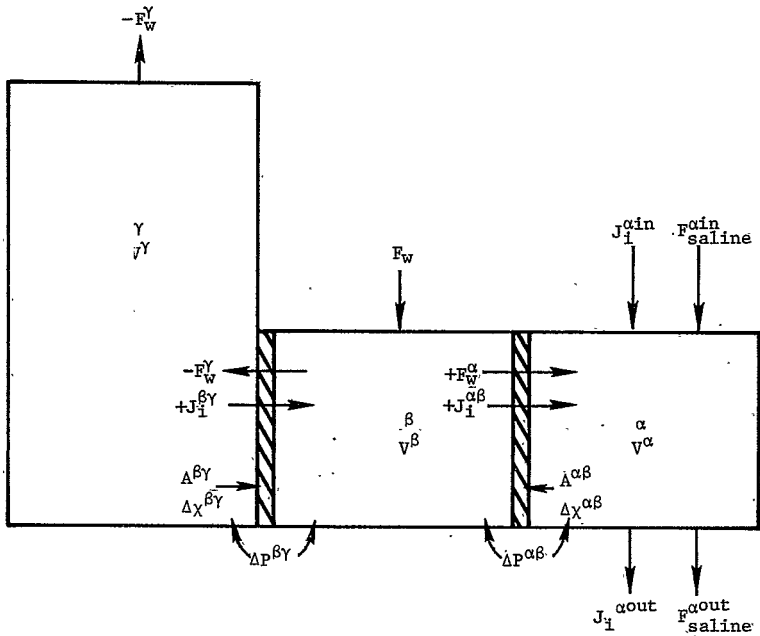
Figure 2.- Steady-State System

compartment, γ. The ion concentrations in compartment γ and in the "lumen" compartment, α, were held constant. The latter was achieved by a constant flow of fixed concentration solution into and out of compartment α. The rate of this flow, and the differences in ion concentrations going into and out of that compartment were a measure of the steady-state ion transport across the membranes for a given unidirectional flow of water from compartments β to γ. Since ion concentrations in compartments α and γ, where experimentally controlled, determination of ion concentrations in the cellular compartment, β, completely defined the nonequilibrium ion distribution for a given flow of water.

This system was also studied under conditions where the flow of water from compartment β could distribute itself into both compartments γ and α.

ANALYTICAL MODEL

The nonequilibrium approaches to ion transport through membranes include thermodynamic as well as mechanical treatments. The former offers the greatest generality, while the latter offers a clearer physical picture of the processes taking place. However, in the case where the membrane is essentially nonselective with regard to the components, one approach has little advantage over the other.

In this investigation, a thermodynamic approach is used. It is an adaptation of Katchalsky and Curran's (19) derivations to include both pressure and concentration gradient forces across a membrane in a multiple solute system. The dissipation function is first written to relate the flows of components and the local chemical potential gradients within the membrane of a two-compartment system. The gradients are then related to the pressures and concentrations within each compartment. Finally, the equations are applied to a two-membrane, three-compartment system.

Consider the two compartment system diagramed in Figure 3 in which the compartments, α and β, are separated by a physical barrier consisting of a membrane of unit area and of thickness Δx. Each compartment contains n solutes and a solvent for a total of $n + 1$ components. At the observation plane, 0, a volume element of unit area and of thickness, dx, can be isolated. We can assume homogeneity and may apply the dissipation function for isothermal diffusion in a continuous phase with $n + 1$ components:
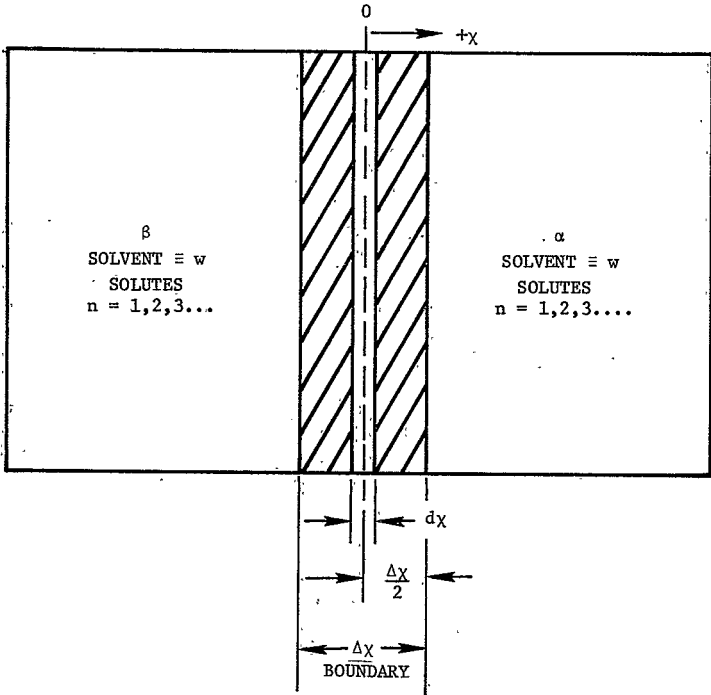
Figure 3.— Two-compartment system

$$22) \qquad \phi = \sum_{i=1}^{n+1} J_i \cdot \text{grad} \ (-\mu_i)$$

ϕ is the dissipation per unit area at plane 0, J_i is the flow per unit area of component i at plane 0, and μ_i is the chemical potential of component i at plane 0.

As derived in Appendix D, equation 22 may be written in terms of the volume flow, J_V, the pressure gradient, grad $(-P)$, the diffusion flow of component i relative to the solvent flow, J_i^d, and the concentration dependent chemical potential gradients, grad $(-\mu_i^c)$.

$$23) \qquad \phi = J_V \ \text{grad} \ (-P) + \sum_{i=1}^{n} J_i^d \ \text{grad} \ (-\mu_i^c)$$

In deriving equation 23, vector notations are dropped since the one-dimensional case is considered, i.e., the flows and forces are only a function of x.

In a stationary state, the flows in equation 23 are constant, and the equation may be integrated across the membrane. The pressure and the chemical potential gradients across the membrane are linear. However, the phenomenological equations defined by the resulting dissipation function involve the phenomenological coefficients, L_{ik}. These coefficients are strong functions of concentration and generally are not available which makes an actual numerical analysis of the theoretical model difficult.

An alternate approach is to write the local phenomenological equations at plane 0 as defined by the dissipation function in equation 23.

24)

$$J_V = - L_P^0 \text{ grad } P - \sum_{k=1}^{n} L_{PD_k} \text{ grad } \mu_k^c$$

$$J_i^d = - L_{DP_i} \text{ grad } P - \sum_{k=1}^{n} L_{ik} \text{ grad } \mu_k^c$$

L_{PD_k} and L_{DP_i} are related to the friction between the membrane and the solutes; that is, they are cross coefficients coupling hydrodynamic flow with diffusional forces and diffusion flows with hydrodynamic forces. They are functions of the permeability and reflection of the membrane to a specific solute. For a very porous membrane, these terms may be neglected; that is,

25)
$$L_{PD} = L_{DP} \approx 0$$

Equations 24 now become the equations for volume flow and diffusional flow, respectively, at plane 0 in an isothermal continuous system:

26)
$$J_V = - L_P^0 \text{ grad } P$$

$$J_i^d = - \sum_{k=1}^{n} L_{ik} \text{ grad } \mu_k^c$$

L_p^0 is the mechanical filtration coefficient for the membrane element and L_{ik} is the coefficient that relates the frictional forces of component i to those of component k at the observational plane, O.

In the case of a stationary state the volume flow, J_V is constant and equation 26 may be integrated across the membrane:

$$27). \qquad\qquad J_V = - L_p \, \Delta P$$

where

$$28) \qquad\qquad \Delta P = P^\alpha - P^\beta$$

L_p is an average filtration coefficient for the membrane.

Equation 26 may be written in terms of diffusion coefficients and concentration gradients:

$$29) \qquad\qquad J_i^d = - \sum_{k=1}^{n} D_{ik} \, \mathrm{grad} \, C_k$$

Equation 29 is similar to the equation for isothermal diffusion in a continuous system derived by Onsager (29).

The diffusional flow, J_i^d, may be written as:

$$30) \qquad\qquad J_i^d = J_i - \frac{C_i}{C_w} J_w$$

where C_w is the concentration of water at plane O and J_w is the flow of water.

The volume flow, J_V, may be written in terms of the solute flows, the water flows, and the partial molar volumes, $\overline{V}_i$ and $\overline{V}_w$:

31)
$$J_V = \sum_{i=1}^{n} \overline{V}_i J_i + \overline{V}_w J_w$$

Derivations of equations 29, 30, and 31 are given in Appendix D.

The solutions may be made sufficiently dilute to make the volume contribution of the solvent, $n_w \overline{V}_w$, to the total volume of the solution, V, overwhelmingly larger than that of the other components such that

32)
$$\overline{V}_w \approx \frac{1}{C_w}$$

Substituting equations 30, 31, and 32 into equations 29 and 27, and multiplying the flows by the total area of the membrane, A, the equations for the flow of component i and the flow of water relative to the membrane at the observational plane are:

$$J_i = \frac{C_i}{C_w} J_w - A \sum_{k=1}^{n} D_{ik} \frac{dC_k}{dx}$$

33)

$$J_w = - C_w A L_p \,\Delta P - \sum_{k=1}^{n} C_w \overline{V}_k J_k$$

Equation 33 states that the flow of solvent is equal to the difference between total flow and solute flow. In the case of bulk flow, the solute flows are negligible relative to the total volume flows. Hence, we may consider the solvent flows being approximately equal to the total volume flow:

34)
$$J_W \approx - C_W AL_P \, \Delta P$$

Combining equations 33 and 34 gives the general equation for the flow of a specific solute as a function of the pressure differential across the membrane, the local concentration gradients and the concentrations of components:

35)
$$J_i = - C_i AL_P \, \Delta P - A \sum_{k=1}^{\overleftrightarrow{}} D_{ik} \frac{dC_k}{dx}.$$

The first term in the equation is the flow of solute i due to the frictional drag effect of the solvent. This phenomenon is sometimes referred to as the frictional cross-coupling effect or solvent drag. It is essentially analogous to the thermal convection phenomenon and may suitably be referred to as the flow of solute due to chemical convection. The last term is the flow of solute i due to diffusional forces. It includes the straight diffusion as described by Fick's law as well as diffusion due to frictional cross-coupling between different solute components. The former flows are related to the forces dC_k/dx by the straight coefficients, D_{ik} (i = k), and the latter flows are related to the forces dC_k/dx by the cross-coupling diffusion coefficients, D_{ik} (i $\neq$ k). These coefficients are only weak functions of concentration at low concentrations and, therefore, are useful in the practical application of equation 35. Values for the coefficients have been given by Dunlop and Gosting (7) by Fujita and Gosting (10) for a ternary system of NaCl - KCl - H_2O. These are listed in Table 1.

As can be seen, the Onsager reciprocal relation for the phenomenological coefficients, $L_{ik} = L_{ki}$, does not apply to the diffusion coefficients.

TABLE 1.- DIFFUSION COEFFICIENTS AT 25° C FOR VARIOUS

CONCENTRATIONS OF A NaCl - KCl - H_2O SYSTEM (7)

NaCl $\equiv$ 1, KCl $\equiv$ 2

C_1 (M) C_2 (M)	0.25 0.25	0.5 0.25	0.25 0.50	0.5 0.5	1.5 1.5
$D_{11} \times 10^5$	1.380	1.433	1.364	1.403	1.464
$D_{12} \times 10^5$	0.011	0.021	0.015	0.026	0.199
$D_{21} \times 10^5$	0.150	0.099	0.207	0.173	0.387
$D_{22} \times 10^5$	1.836	1.831	1.863	1.859	1.901

In order to apply equation 35 it is necessary to define the local concentrations and concentration gradients for all components at the observational plane in terms of the concentrations in the compartments on either side of the membrane. This is difficult to do since both the concentration and concentration gradient at any point in time vary as a function of pore size, pore distribution, and solution agitation. The concentrations within the membrane are difficult to measure. It is necessary to assume a gradient, calculate the resulting concentrations within the compartments and compare this to experimental data. This has been done by Ekman, Rastas, and Salminen (8, 33) on a system of NaCl - KCl - HCl - H_2O for two compartments connected by a capillary pore.

A concentration gradient term may be developed from equation 35, if we assume the gradient results from two conditions: first, no pressure gradients exist throughout the system, i.e., $- AL_p \Delta P = F_W = 0$; second, the system is in a stationary state of the first order where only the flow of water exists, i.e., $J_i = 0$, $F_W \neq 0$. The concentrations of components at the surface of the membrane are assumed equal to the concentrations within the compartments bordering that membrane surface, i.e., $C_i(x = 0) = C_i^\beta$, $C (x = \Delta x) = C_i^\alpha$. For the stationary state we may integrate equation 35 for the listed conditions:

36)
$$C_i(F_W = 0) = c_i^\alpha + (c_i^\beta - c_i^\alpha)\left(\frac{\Delta x - x}{\Delta x}\right)$$

$$C_i(J_i^{\alpha\beta} = 0) = c_i^\alpha e^{F_W(x - \Delta x)/AD_{ii}^*}$$

The asterisked diffusion coefficients denote that an average value was taken over the concentration range integrated. Cross-coupling terms have been neglected for deriving equation 36. The validity of dropping the cross-coefficients is demonstrated in Appendix D.

Combining equations 36 gives a generalized equation for the concentration of component i as a function of distance x within the membrane:

$$C_i(x) = C_i^{\alpha}e^{F_w(x-\Delta x)/AD_{ii}^*} + \left(C_i^{\beta} - C_i^{\alpha}e^{-F_w\Delta x/AD_{ii}^*}\right)\left(\frac{\Delta x - x}{\Delta x}\right)$$

37)

$$\frac{dC_i(x)}{dx} = \frac{F_w C_i^{\alpha}}{AD_{ii}^*}e^{F_w(x-\Delta x)/AD_{ii}^*} - \left(\frac{C_i^{\beta} - C_i^{\alpha}e^{-F_w\Delta x/AD_{ii}^*}}{\Delta x}\right)$$

Let

38)
$$b_{ik} \equiv \frac{AD_{ik}^*}{\Delta x}$$

When $x = \Delta x/2$, the equations for concentration and concentration gradients become:

$$C_i\left(x = \frac{\Delta x}{2}\right) = C_i^{\alpha}e^{-F_w/2b_{ii}} + \frac{\left[C_i^{\beta} - C_i^{\alpha}e^{-F_w/b_{ii}}\right]}{2}$$

39)

$$\frac{dC_i}{dx}\left(x = \frac{\Delta x}{2}\right) = F_w b_{ii} C_i^{\alpha}e^{-F_w/2b_{ii}} - \frac{\left[C_i^{\beta} - C_i^{\alpha}e^{-F_w/b_{ii}}\right]}{\Delta x}$$

Equations 35 and 39 may be applied to the two-membrane, three-compartment system shown in Figure 1. The components are defined as follows: $NaCl \equiv 1$, $KCl \equiv 2$, $H_2O \equiv w$. A pressure differential, ΔP, between compartment β and γ is established by the constant addition of water to compartment β and the constant removal of water from compartment γ at a rate $F_w^{\gamma} = - (AL_p \Delta P)^{\beta\gamma}$.

The specific volumes of the compartments remain approximately constant. Compartment α is essentially closed to volume flow. The volumes of compartments β and γ likewise remain constant in that the amount of solvent entering is equal to the amount leaving. Consequently, the changes in concentrations of components within the compartments is due only to solute flow leaving and entering. For compartment α, a positive rate of change in the amount of component i is equal to the flow of i into α, or

40)
$$\frac{dn_i^\alpha}{dt} = V^\alpha \frac{dC_i^\alpha}{dt} = J_i^{\alpha\beta}$$

J_i is constant throughout the membrane.

For compartment γ, a positive rate of change in the amount of component i is equal to the flow of i into γ, or in the negative x direction:

41)
$$\frac{dn_i'}{dt} = V^\gamma \frac{dC_i'}{dt} = - J_i^{\beta\gamma}$$

For compartment β, a positive rate of change in the amount of component i is equal to the difference of the flow of i out of γ and out of α:

42)
$$\frac{dn_i^\beta}{dt} = V^\beta \frac{dC_i^\beta}{dt} = J_i^{\beta\gamma} - J_i^{\alpha\beta} = - V^\gamma \frac{dC_i'}{dt} - V^\alpha \frac{dC_i''}{dt}$$

Combining equations 35, 39, 40, 41, and 42, and taking into consideration that $F_W^\alpha = - (AL_p \Delta P)^{\alpha\beta} = 0$ for the nonsteady-state model, we obtain a system of differential equations defining the concentration of each component in each compartment at every point in time.

$$V^\alpha \frac{dC_1^\alpha}{dt} = - b_{11}^{\gamma\beta}C_1^\alpha - b_{12}^{\alpha\beta}C_2^\alpha + b_{11}^{\alpha\beta}C_1^\beta + b_{12}^{\alpha\beta}C_2^\beta$$

$$V^\alpha \frac{dC_2^\alpha}{dt} = - b_{21}^{\alpha\beta}C_1^\alpha - b_{22}^{\alpha\beta}C_2^\alpha + b_{21}^{\alpha\beta}C_1^\beta + b_{22}^{\alpha\beta}C_2^\beta$$

$$\frac{V^\alpha}{V^\beta} \frac{dC_1^\alpha}{dt} + \frac{dC_1^\beta}{dt} + \frac{V^\gamma}{V^\beta} \frac{dC_1^\gamma}{dt} = 0$$

$$\frac{V^\alpha}{V^\beta} \frac{dC_2^\alpha}{dt} + \frac{dC_2^\beta}{dt} + \frac{V^\gamma}{V^\beta} \frac{dC_2^\gamma}{dt} = 0$$

43)

$$V^\gamma \frac{dC_1^\gamma}{dt} = \left(- \frac{F_W^\gamma}{2} + b_{11}^{\beta\gamma} \right)C_1^\beta + b_{12}^{\beta\gamma}C_2^\beta + \left(\frac{F_W^\gamma}{2} - b_{11}^{\beta\gamma} \right)e^{F_W^\gamma/b_{11}^{\beta\gamma}} C_1^\gamma$$

$$+ \left(F_W^\gamma \frac{b_{12}^{\beta\gamma}}{b_{22}^{\beta\gamma}} e^{F_W^\gamma/2b_{22}^{\beta\gamma}} - b_{12}^{\beta\gamma}e^{F_W^\gamma/b_{22}^{\beta\gamma}} \right)C_2^\gamma$$

$$V^\gamma \frac{dC_2^\gamma}{dt} = b_{21}^{\beta\gamma}C_1^\beta + \left(- \frac{F_W^\gamma}{2} + b_{22}^{\beta\gamma} \right)C_2^\beta + \left(F_W^\gamma \frac{b_{21}^{\beta\gamma}}{b_{11}^{\beta\gamma}} e^{F_W^\gamma/2b_{11}^{\beta\gamma}} \right.$$

$$\left. - b_{21}^{\beta\gamma}e^{F_W^\gamma/b_{11}^{\beta\gamma}} \right)C_1^\gamma + \left(\frac{F_W^\gamma}{2} - b_{22}^{\beta\gamma}e^{F_W^\gamma/b_{22}^{\beta\gamma}} \right)C_2^\gamma$$

The above equations are a system of linear, first-order equations. Solutions of these equations are of the type (35):

44)
$$C_i = K_o + k_o t + \sum_{j=1}^{4} K_{ij} e^{\lambda_j t} .$$

Time histories of the concentrations using specific coefficients and initial conditions in equations 43 have been produced by computer program and are presented under Results. The program also produced the specific eigenvalues, λ_i, and eigenvectors, K_{ij}, for equation 44.

The concentrations in all three compartments change with time until a stationary condition is reached. This occurs when $c_i^\alpha = c_i^\beta$, at which point the system effectively becomes a two-compartment system. In order to investigate a steady-state in a three-compartment system, it is necessary to hold constant the concentration of components in two of the three compartments.

The concentrations of components in compartment α are now held constant by a constant flow of solution with fixed component concentration into and out of compartment α. The concentrations of components in compartment γ are maintained approximately constant by making the compartment volume extremely large compared to compartments α and β. This system is shown in Figure 2.

In this system, the concentrations of components in compartment α will reach steady-state values different from those in compartment β. At steady-state, the rate of change of component i in compartment α is zero, or from equation 40

$$V^\alpha \frac{dC_i^\alpha}{dt} = J_i^{\alpha out} - J_i^{\alpha in} - J_i^{\alpha\beta} = 0$$

. 45)

$$\Delta J_i^\alpha = J_i^{\alpha out} - J_i^{\alpha in} = J_i^{\alpha\beta}$$

ΔJ_i^α is the steady-state transport of component i into and out of compartment α

In the steady-state case, the rate of change of components in each compartment is zero and, consequently, all flows are constant throughout the system:

. 46)
$$J_i^{\beta\gamma} = J_i^{\alpha\beta} = \Delta J_i^\alpha .$$

Substituting equation (46) into equation (35), and utilizing the concentration gradient from equations 39, we can develop the equations defining the steady state transport of components 1 and 2 between compartments α and γ:

$$\cdot \Delta J_1^\alpha = -\left[\frac{F_w^\alpha}{2} + b_{11}^{\alpha\beta}\right]e^{-F_w^\alpha/b_{11}^{\alpha\beta}} C_1^\alpha - \left[\frac{F_w b_{12}^{\alpha\beta}}{b_{22}^{\alpha\beta}} e^{-F_w^\alpha/2b_{22}^{\alpha\beta}} + b_{12}^{\alpha\beta}e^{-F_w^\alpha/b_{22}^{\alpha\beta}}\right]C_2^\alpha$$

$$+ \left[\frac{F_w^\alpha}{2} + b_{11}^{\alpha\beta}\right]C_1^\beta + \left[b_{12}^{\alpha\beta}\right]C_2^\beta$$

$$\Delta J_2^\alpha = -\left[F_w^\alpha \frac{b_{21}^{\alpha\beta}}{b_{11}^{\alpha\beta}} e^{-F_w^\alpha/2b_{11}^{\alpha\beta}} + b_{21}^{\alpha\beta}e^{-F_w^\alpha/b_{11}^{\alpha\beta}}\right]C_1^\alpha - \left[\frac{F_w^\alpha}{2} + b_{22}^{\alpha\beta}\right]e^{-F_w^\alpha/b_{22}^{\alpha\beta}} C_2^\alpha$$

$$+ \left[b_{21}^{\alpha\beta}\right]C_1^\beta + \left[\frac{F_w^\alpha}{2} + b_{22}^{\alpha\beta}\right]C_2^\beta$$

47)

$$\Delta J_1^\alpha = \left[\frac{F_w^\gamma}{2} - b_{11}^{\beta\gamma}\right]c_1^\beta + \left[- b_{12}^{\beta\gamma}\right]c_2^\beta + \left[- \frac{F_w^\gamma}{2} + b_{11}^{\beta\gamma}\right]e^{F_w^\alpha/b_{11}^{\beta\gamma}} c_1^\gamma$$

$$\quad + \left[- \frac{F_w^\gamma b_{12}^{\beta\gamma}}{b_{22}^{\beta\gamma}} e^{F_w^\gamma/2b_{22}^{\beta\gamma}} + b_{12}^{\beta\gamma} e^{F_w^\gamma/b_{22}^{\beta\gamma}}\right]c_2^\gamma$$

$$\Delta J_2^\alpha = \left[- b_{21}^{\beta\gamma}\right]c_1^\beta + \left[\frac{F_w^\gamma}{2} - b_{22}^{\beta\gamma}\right]c_2^\beta + \left[- \frac{F_w^\gamma b_{21}^{\beta\gamma}}{b_{11}^{\beta\gamma}} e^{F_w^\gamma/2b_{11}^{\beta\gamma}}\right.$$

$$\quad \left. + b_{21}^{\beta\gamma} e^{F_w^\gamma/b_{11}^{\beta\gamma}}\right]c_1^\gamma + \left[- \frac{F_w^\gamma}{2} + b_{22}^{\beta\gamma}\right]e^{F_w^\gamma/b_{22}^{\beta\gamma}} c_2^\gamma$$

The above four simultaneous equations have four unknowns: the transport of NaCl and of KCl, and the concentrations of NaCl and of KCl in compartment β. Solutions obtained by computer program for specific conditions and coefficients are given under Results.

APPARATUS

The basic experimental apparatus used consisted of three liquid
compartments separated by porous membranes as shown in Figure 4. The
compartments were formed by clamping two hollow Lucite blocks to a
large Lucite box with four threaded rods. The blocks were 2 in.
by 2 in. by 2.25 in., and were bored with a center hole of 3/4 in.
diameter. The small compartments, α and β, were cylindrical.
Compartment β had a porous membrane on either end and compartment α
had a porous membrane only on one end. The volumes of compartments α
and β were 14 cc each. The Lucite box, compartment γ, was 7 in. by
7 in. by 6 in. Its volume was approximately 4 liters. On one side,
the box had a 3/4 in. diameter hole and an adapter for clamping
compartments α and β. On two other sides, the box had 5 in. diameter
openings and bolt holes for clamping membranes and attaching salt
compartments for the osmotic removal of water from compartment γ as
shown in Figure 5. A more detailed description of the apparatus may
be found in Appendix A.

The entire apparatus was submerged in a Lucite water bath. All
tubes from the apparatus extended through the surface of the water
bath. Two sampling ports to compartments α and β extended through
the front of the water bath. The temperature of the water bath was
maintained at 25° C by a constant temperature circulating system
(Precision Instrument Co., model 66600).
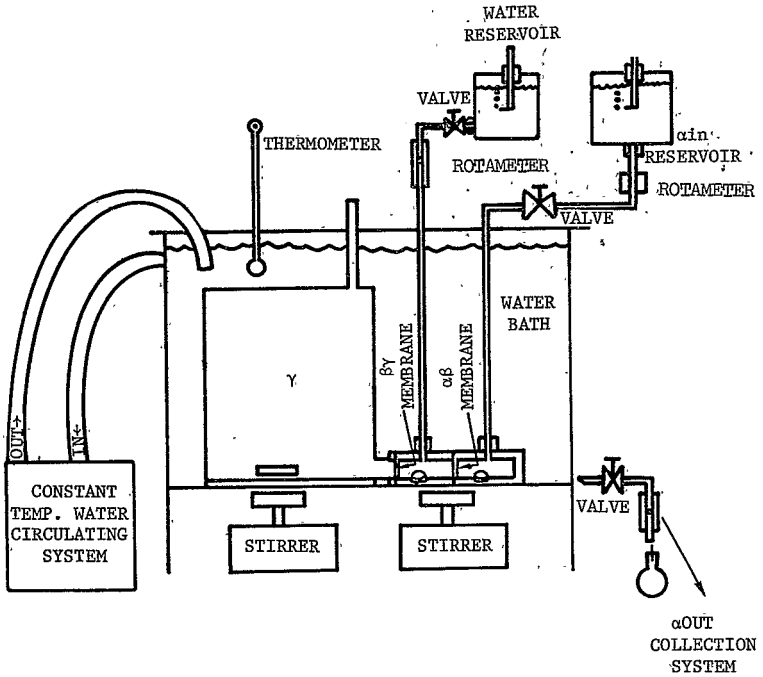
Figure 4.- Experimental Apparatus.
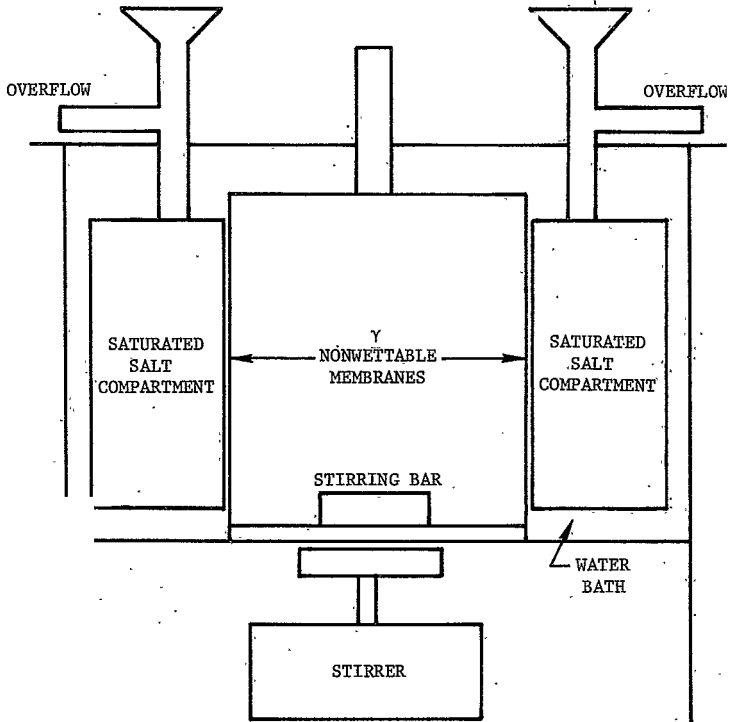
Figure 5.- Cross section through compartment γ.

The solutions were agitated at a constant rate by two magnetic stirrers (Thomas Co., model 15). One stirrer agitated compartments α and β by means of two 1/2 in. diameter Teflon-coated stirring balls. The other stirrer agitated compartment γ by means of a 1-1/2 in. Teflon coated stirring bar.

Pressures within compartments α and β were determined by capillary manometer tubes extending from the rear of the compartments. Hydrostatic pressure within compartment γ was determined by the liquid level within a fill tube extending from the top of the compartment.

Water feed into compartment β and NaCl - KCl solution feed into compartment α was accomplished by hydrostatic feed from reservoirs. The hydrostatic heads of the reservoirs were held constant by permitting makeup air at atmospheric pressure to bleed into the reservoirs through tubes at the bottoms of the reservoirs. The air bleed tubes consisted of glass tubes with hypodermic needles bent horizontally to maintain an even, small-bubble flow of air into the reservoir. The heights of the reservoirs were adjustable. The liquid flowed through rotameter-type flowmeters (Manostat, model 36-541-05) into the top sides of compartments α and β (Figure 4).

The constant outflow of solution from compartment α in the steady state experiments was accomplished by means of a hypodermic needle pierced through a rubber septum on the front side of the compartment. Polyethylene capillary tubing connected the hypodermic needle to a rotameter. Flow was controlled by adjusting the total head from

reservoir air-bleed level to collecting point and by the back pressure sustained by a hypodermic needle at the solution collecting point.

Flow of water into compartment β and across the βγ membrane was controlled by the difference in pressure between the total hydrostatic head to the membrane and the liquid level in compartment γ. The latter was controlled by the rate of osmotic outflow of water from that compartment. Thus the water flow proceeded at the demand rate dictated by the osmotic water outflow from compartment γ. The osmotic water outflow was accomplished by nonwettable vinyl fluoride membranes (Gelman, VF type) separating compartments γ from adjacent compartments filled with saturated salt solutions (Figure 5). Water removal rates were varied by changing the total membrane area and by employing different salts in the saturated salt compartments. NaCl, CaCl$_2$, and LiCl produced water flows in respectively increasing magnitudes for the same membrane area. The saturated salt solutions were permitted to overflow into a collecting container. Saturation was maintained by keeping an abundance of undissolved salt within the osmotic chambers. The utilization of the nonwettable membranes for creating osmotic flows of water is discussed in Appendix A.

Sampling of solutions from compartments α and β was accomplished by using 100 μL syringes to withdraw samples through a rubber septum fitted into the front side of each of these compartments (Figure 6). Sampling from compartment γ was done through a 1/2 in. diameter filling tube extending from the top of that compartment.
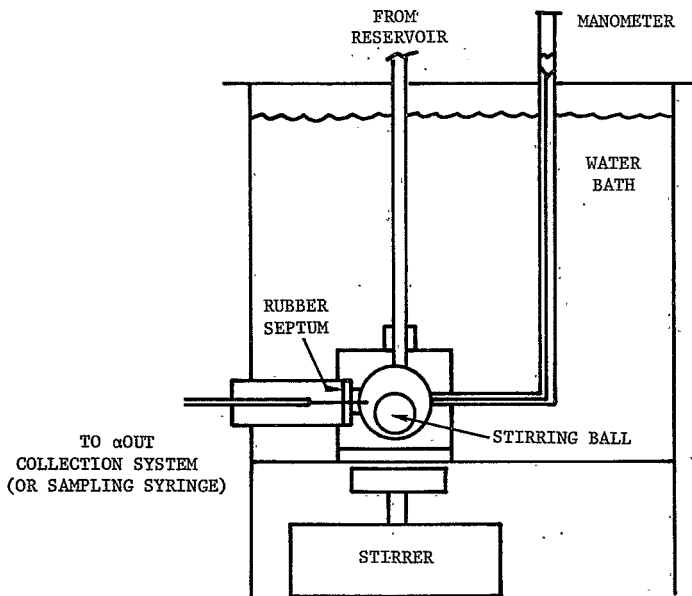
Figure 6.- Cross section of compartment α or β.

The porous membranes used in this investigation were commercially available membrane filters. They consisted of Millipore types GS and VC, and Gelman type GA-9. The manufacturers' specifications for these membranes are given in Table 2. The filters were cut to a diameter of 1-1/8 in. The actual area exposed to the liquid phases was 4.57 cm^2.
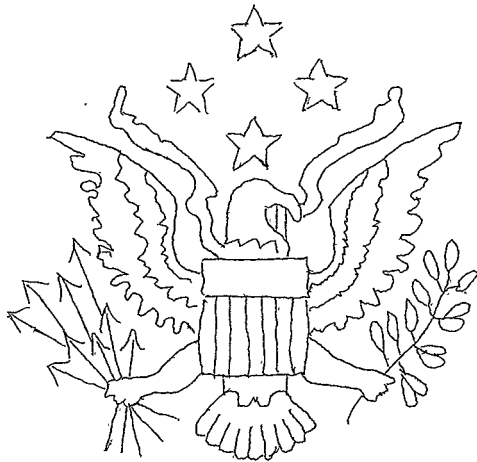
TABLE 2.- SPECIFICATIONS FOR MEMBRANE FILTERS (2, 42)

Type	Composition	Pore size	Thickness	Porosity	Water flow rate at $\Delta P = 700$ mm of Hg
Gelman GA-9	Cellulose triacetate	0.10μ	$127 - 152\mu$	85 percent	$4(ml/min)/cm^2$
Millipore VC	Mixed esters of cellulose	$0.10 \pm 0.008\mu$	$130 \pm 10\mu$	74 percent	$2(ml/min)/cm^2$
Millipore GS	Mixed esters of cellulose	$0.22 \pm 0.02\mu$	$135 \pm 10\mu$	75 percent	$21 \pm 3 \ (ml/min)/cm^2$

PROCEDURES

Nonsteady-State Experiments

Either Millipore GS or Gelman GA-9 type membranes were used in the $\beta\gamma$ position. Gelman GA-9 type membranes were used in the $\alpha\beta$ position. The latter membranes have a low mechanical filtration coefficient which reduced the amount of solution mixing between the α and β compartments during filling. This maintained the initial compartment α ion concentrations close to the ultimate steady state values and reduced the time to reach stationary state conditions.

Compartment γ was filled with NaCl - KCl solution ranging from 98 to 160 mM. Compartment α was filled with NaCl - KCl solutions ranging from 5 to 8 mM. The initial solution in compartment β consisted of solution from compartment γ flowing through the $\beta\gamma$ membr during filling plus an addition of distilled water to fill the compartment. No attempt was made to control the initial concentrations in compartment β.

The apparatus was "brought to life" by filling the osmotic chambers with saturated salt solution and opening a valve in the reservoir-to-compartment β water line. The water flow rate adjusted itself automatically as the water inflow and osmotic outflow equilibrated. Various flow rates, ranging from 0.07 to 0.300 ml/min, were established by a combination of one or two osmotic chambers, and saturated NaCl, $CaCl_2$, or LiCl solutions.

The water bath temperature was adjusted to 25° C and maintained within $\pm 0.5^\circ$ C. Constant stirring was maintained. A 100 µL sample was taken out of each compartment immediately. Samples were then taken hourly for the first few hours and then every 2 to 3 hours for the remainder of the experiment. No samples were taken for a period of 6 to 8 hours during each night of the experiment. Each experiment required 2 to 3 days to reach stationary state. Flow rates and temperature readings were taken at each sampling.

Samples were diluted to a range of 0.025 to 0.2 mM. This was the linear range of Na^+ and K^+ concentrations as a function of optical density for the Beckman Atomic Absorption system employed. Cl^- activity was first measured with an Ag/AgCl electrode and a Beckman research pH meter. Na^+ and K^+ concentrations were determined by atomic absorption spectrophotometry and standardization curves. These curves were obtained periodically from a series of gravimetrically derived NaCl and KCl standard solutions.

Steady-State Experiments

The membrane in the $\beta\gamma$ position consisted of the Millipore GS type membrane. In the initial experiments water flow into compartment β was permitted only across the $\beta\gamma$ membrane into compartment γ. This was accomplished by using the Millipore VC type membrane which has a low mechanical filtration coefficient and maintaining a near zero pressure differential across the $\alpha\beta$ membrane. The water bath was maintained at $25.0 \pm 0.1^\circ$ C.

In later experiments, Millipore GS type membranes were used in both the $\alpha\beta$ and $\beta\gamma$ positions. In these experiments the flow of water into compartment β partially distributed into the α compartment depending on the magnitude of the pressure differential across the $\alpha\beta$ membrane

The apparatus was filled as in the nonsteady-state experiments. The NaCl and KCl concentrations of the filling solutions for compartment γ were maintained at approximately 100 mM throughout these experiments. A set of experiments was run over a range of water flows into β from 0 to 0.7 ml/min for each of the following NaCl - KCl concentrations of solution flowing into α: 100 mM, 50 mM, 25 mM, and 5 mM. Each solution brought about an increasing concentration gradient in compartment α relative to compartment β.

In initial experiments water flows into β and out of γ were controlled as in the nonsteady-state experiments, that is, by hydro-static feed into β and osmotic removal from γ. In later experiments total water flow into compartment β also depended on the pressure differential across the $\alpha\beta$ membrane.

Solution flow rate through compartment α was controlled by the hydrostatic head and back pressure from the collecting needle. This flow was so controlled as to maintain a constant measurable con-centration differential between the in and outflow for a solution of given concentration flowing into α. The intent was to maintain a constant concentration gradient from α to γ for a given solution flowing into α over the entire water flow range into the β compartment.

This then permitted a plot of ion transport against a constant concentration gradient versus water flow.

The system reached a steady-state by running overnight. Timed samples of compartment α outflow were collected in 10 ml volumetric flasks and 100 μL samples were taken from both β and γ. Flows α_{in}, α_{out}, β_{in}, and the temperature were recorded. Samples were taken until three consecutive samples had the same ion concentrations which indicated that the system had reached a steady-state.

Sampling, dilutions, and analyses were performed as in the nonsteady-state experiments. In addition, gravimetric determinations of total salt content in the α_{in} and α_{out} samples were made. The ion transport rates were calculated as given in Appendix C.

RESULTS AND DISCUSSION

Initial comparisons of theoretical and experimental results made it immediately apparent that correlation of the data with the theoretical predictions depended highly on the assumed values of the effective membrane pore areas and gradient boundary thickness. There are a number of reasons for this. First, in the theoretical derivations, phenomena related to the actual existence of pores within the membranes and to the tortuosity would have the effect of decreasing the effective pore area and increasing the boundary thickness. Second, solution stirring has a significant effect on boundary thickness. Because of the apparatus design, the stirring for these experiments was only moderately controlled. The geometry of the apparatus and the use of a water bath for temperature control necessitated the use of magnetic stirrers and relatively small stirring bars or balls, which proved to be only a moderately effective method of solution agitation. Also, the apparatus design was such that there existed a poorly stirred region on the γ compartment side of the $\beta\gamma$ membrane. All this had the effect of increasing the boundary thickness. Finally, each experiment was conducted over a period of days during which time the membranes became partially clogged. Although the hydrostatic head was increased to maintain constant water flow, the effect of the clogging was to decrease effective membrane pore area. Similar membrane clogging was observed by Nims and Thurber (26.). The problem of not being able to precisely specify the membrane effective pore areas and boundary thicknesses, necessitated the introduction of an empirical

parameter, η, correlating theoretical values to the manufacturer's membrane specifications:

$$48) \qquad \eta = \frac{\left(\frac{A}{\Delta x}\right)_{\text{theoretical}}}{\left(\frac{A}{\Delta x}\right)_{\text{manufacturers' specs}}}$$

A comparison of the experimental data for the time rate of change of Na^+ and K^+ concentrations in compartments α and β, shown in Figure 10 and Table 4, with the theoretical results, shown in Figure 9, for the same water flow rate across the $\beta\gamma$ membrane indicates that the ratios of membrane area to boundary thickness were less than the membrane manufacturer's values.

An additional problem in correlating experimental data to theoretical calculations was the difficulty of specifying the velocity of water molecules within the membrane. The analytical model neglected viscous effects near the pore walls and assumed a constant water velocity equal to the water flow across the membrane per unit pore area. The assumptio of a velocity was difficult because of the difficulty in specifying the pore area. A decrease in pore area has the effect of increasing the water velocity. Furthermore, in the case of viscous flow through a cylindrical pore, the flow is of the Hagen-Poiseuille type (1) in which relatively static layer of fluid, existing along the pore wall, decrease the effective pore area and therefore increases the average water velocity. Pore tortuosity increases this effect still further. This difficulty made it necessary to introduce another empirical parameter, θ, correlating the theoretical average water velocity within the

membrane to the experimental water flux:

49)
$$\theta = \frac{\left(v_w\right)_{theoretical}}{\left(\frac{F_w}{A}\right)_{experimental}}$$

η and θ are functions of the membrane pore area. η is a function of the area through which diffusion occurs and θ is a function of the area through which bulk flow occurs. These areas need not necessarily be the same.

Three nonsteady-state cases of ion concentration variation with time in compartments α and β are given below. In each case the initial concentration of each ion in compartment β is greater than that in compartment α. In the first case a low water flow rate, F_w^γ, is utilized. The concentrations of both Na^+ and K^+ in compartment α increase with time until a stationary state is reached. This increase is due to the transient transport of the ions down concentration gradients from compartment γ to compartment α. The theoretical and experimental results are given in Figure 7 and Table 3. In the second case, a higher water flow rate, F_w^γ, was used. The concentration of K^+ in compartment α again increases with time. However, the Na^+ concentration in compartment α behaves differently. After a time equal to $t_{Na^+}^O$, when the Na^+ concentrations in compartments α and β are equal, the Na^+ concentration in compartment α decreases until a stationary state is reached. Since the Na^+ concentration in compartment β is decreasing simultaneously, the Na^+ leaving compartment α enters compartment γ, which has a Na^+ concen- tration an order of magnitude greater than that of α. The net effect is

Figure 7.- Theoretical variation of Na^+ and K^+ concentrations in compartments α and β with time. $F_w^\gamma = -0.100$ ml/min, $\eta^{\alpha\beta} = 0.217$, $\eta^{\beta\gamma} = 0.217$, $C_{Na^+}^\gamma = 140$ mM, $C_{K^+}^\gamma = 150$ mM. Note increase of $C_{Na^+}^\alpha$ and $C_{K^+}^\alpha$ with time indicating transport of these ions from γ to α down concentration gradients. Stationary state K^+ concentrations are greater than Na^+ concentrations.

TABLE 3.- NONSTEADY-STATE EXPERIMENT (NO. 10); $\alpha\beta$ and $\beta\gamma$

MEMBRANES $\equiv$ GELMAN GA-9,

$C_{Na}^{\gamma}+$ = 123 mM, $C_K^{\gamma}+$ = 99 mM, $C_{Cl}^{\gamma}-$ = 222 mM

Time	F_w^{γ}	Temp.	$C_{Na}^{\alpha}+$	$C_{Na}^{\beta}+$	$C_K^{\alpha}+$	$C_K^{\beta}+$	$C_{Cl}^{\alpha}-$	$C_{Cl}^{\beta}-$
hr	ml/min	°C	mM	mM	mM	mM	mM	mM
0	-0.068	22.0	2.50	22.3	2.80	14.9	5.30	37.2
1	-0.072	25.3	4.70	17.5	5.70	16.8	10.4	34.3
2	-0.075	25.6	6.70	14.2	7.70	16.5	14.4	30.7
4	-0.075	26.6	8.30	13.1	10.6	17.0	18.9	30.1
6	-0.075	28.1	--	13.4	--	18.1	--	31.5
8	-0.076	28.0	10.2	14.0	15.0	18.6	25.2	32.6
11	-0.075	28.0	11.8	14.3	17.2	19.7	29.0	34.0
14	-0.075	28.0	12.8	14.9	18.4	20.6	31.2	35.5
17	-0.075	28.0	13.8	15.0	19.2	19.9	33.0	34.9
23	-0.075	28.0	15.2	17.0	21.0	21.6	36.2	38.6
26	-0.075	28.0	15.3	16.5	21.0	21.6	36.3	39.1
29	-0.075	28.0	15.8	16.6	21.2	22.0	37.0	38.6
32	-0.075	28.0	16.8	17.7	21.6	21.6	38.4	39.3
48	-0.080	28.0	18.1	15.9	23.3	23.4	41.4	39.3
50	-0.077	28.0	16.8	16.9	21.6	22.9	38.4	39.8
54	-0.080	28.0	17.6	17.4	23.0	22.9	40.6	40.3

a transient transport of K^+ down a concentration gradient and a simul-
taneous transient movement of Na^+ in the opposite direction against a
much greater concentration gradient. Attempts to demonstrate this case
experimentally were unsuccessful because the necessary water flow rates
and initial concentrations were in a difficult to control narrow range.
The theoretical results are shown in Figure 8. In the third case (Figs.
9, 10, and Table 4) even larger water flow rates, F_w^γ, were used. The
concentrations of Na^+ and K^+ in compartment α decrease after time equal
to $t_i^{\,0}$. Both Na^+ and K^+ now demonstrate a transient movement from
compartment α to compartment γ against a concentration gradient.
Additional experimental data demonstrating the third case are given,
Appendix B.

Results of the nonsteady-state experiments demonstrated the tendency
for the concentration of K^+ to be higher than that of Na^+ in compartment
β, the "cellular" compartment. Values of the Nims' distribution function
are shown in Table 5. Values calculated from the experimental conditions
at stationary state compare reasonably well with the expected value
of 1.2. Values of the function calculated from the theoretical data
were almost in all cases precisely 1.2.

Results of the steady-state experiments in which the water flow
rate across the $\alpha\beta$ membrane was zero are given in Table 6 and in Fig-
ures 11-16. Each pair of figures represents data for transport against
consecutively increasing concentration gradients from compartment α to
compartment γ: C_i^γ/C_i^α = 1.11 to 1.17, C_i^γ/C_i^α = 2.11 to 2.41, and
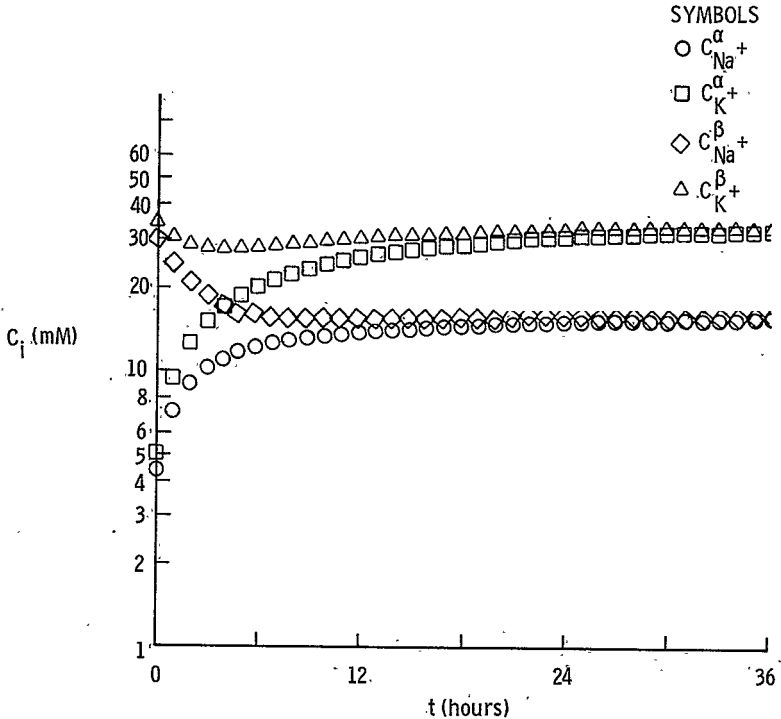C_i^γ/C_i^α = 4.00 to 5.15.
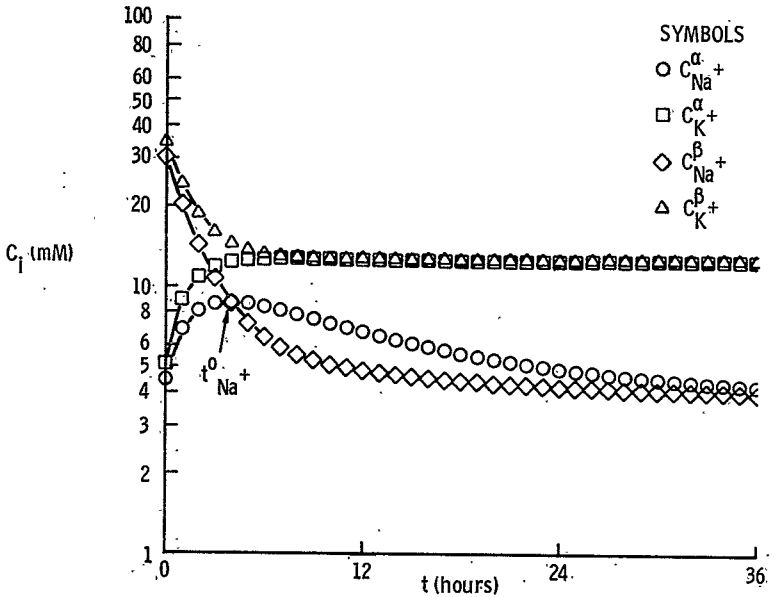
Figure 8.- Theoretical variation of Na^+ and K^+ concentrations in
compartments α and β with time. $F_w^\gamma = -0.167$ ml/min,
$\eta^{\alpha\beta} = 0.217$, $\eta^{\beta\gamma} = 0.217$, $C_{Na^+}^\gamma = 140$ mM, $C_{K^+}^\gamma = 150$ mM.
Note that $C_{K^+}^\alpha$ is increasing with time indicating K^+
transport from γ to α down a concentration gradient
while $C_{Na^+}^\alpha$ is decreasing after $t_{Na^+}^0$ indicating Na^+
transport from α to γ against a concentration gradient
Stationary state K^+ concentrations are greater than Na^+
concentrations.
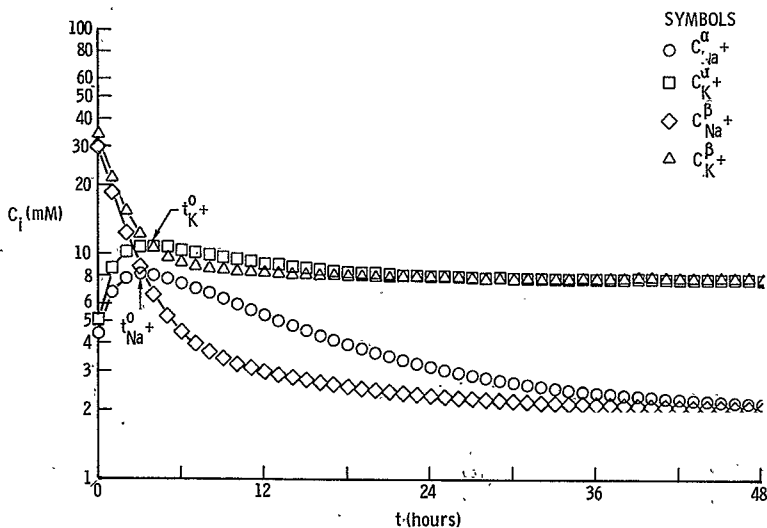
Figure 9.- Theoretical variation of Na^+ and K^+ concentrations i
compartments α and β with time. $F_w^{\gamma} = -0.198$ ml/min,
$\eta^{\alpha\beta} = 0.217$, $\eta^{\beta\gamma} = 0.217$, $c_{Na^+}^{\gamma} = 140$ mM, $c_{K^+}^{\gamma} = 150$ mM.
Note that both $c_{Na^+}^{\alpha}$ and $c_{K^+}^{\alpha}$ increase after t_i^0 indicating
transport from α to γ against concentration gradients.
Stationary state K^+ concentrations are greater than Na^+
concentrations.

TABLE 4.- NONSTEADY-STATE EXPERIMENT (NO. 7); $\alpha\beta$ MEMBRANE $\equiv$ GELMAN GA-9;

$\beta\gamma$ MEMBRANE $\equiv$ MILLIPORE GS

$c_{Na^+}^\gamma = 130$ mM, $c_{K^+}^\gamma = 120$ mM, $c_{Cl^-}^\gamma = 250$ mM

| Time	F_w^γ	Temp.	$c_{Na^+}^\alpha$	$c_{Na^+}^\beta$	$c_{K^+}^\alpha$	$c_{K^+}^\beta$	$c_{Cl^-}^\alpha$	$c_{Cl^-}^\beta$
hr	cc/min	°C	mM	mM	mM	mM	mM	mM
0.	0	23.7	7.00	45.3	7.00	45.0	14.0	90.3
0.75	-0.187	24.8	9.40	17.5	9.60	19.5	19.0	37.0
1.75	-0.187	25.4	9.80	8.70	9.90	16.3	19.7	25.0
3.25	-0.187	25.1	--	4.90	--	8.20	--	13.1
4.75	-0.192	24.9	9.00	5.50	10.0	7.50	19.0	13.0
6.75	-0.195	25.0	7.30	3.70	8.80	7.20	16.1	10.9
9.25	-0.199	25.0	6.20	3.40	9.40	8.10	15.6	11.5
12.25	-0.199	25.0	4.80	3.10	8.80	8.90	13.6	12.0
15.25	-0.192	25.0	4.50	2.80	7.20	6.80	11.7	9.60
22.75	-0.185	25.0	4.00	3.70	7.00	7.70	11.0	11.4
23.75	-0.187	25.0	3.80	3.80	6.90	7.10	10.7	10.9
25.25	-0.187	25.0	3.90	3.70	7.00	7.50	10.9	11.2
27.25	-0.187	25.0	3.90	3.80	7.50	7.80	11.4	11.6
29.25	-0.187	25.1	--	3.70	--	7.30	--	11.0
30.25	-0.187	25.0	3.60	3.70	7.70	8.50	11.3	12.2
31.25	-0.187	25.0	3.60	3.60	8.00	8.10	11.6	11.7
47.50	-0.183	25.0	3.70	3.80	8.20	8.60	11.9	12.4
49.25	-0.183	25.0	3.80	4.20	8.40	9.20	12.2	13.4
54.25	-0.183	25.0	3.80	3.80	8.20	8.10	12.0	11.9
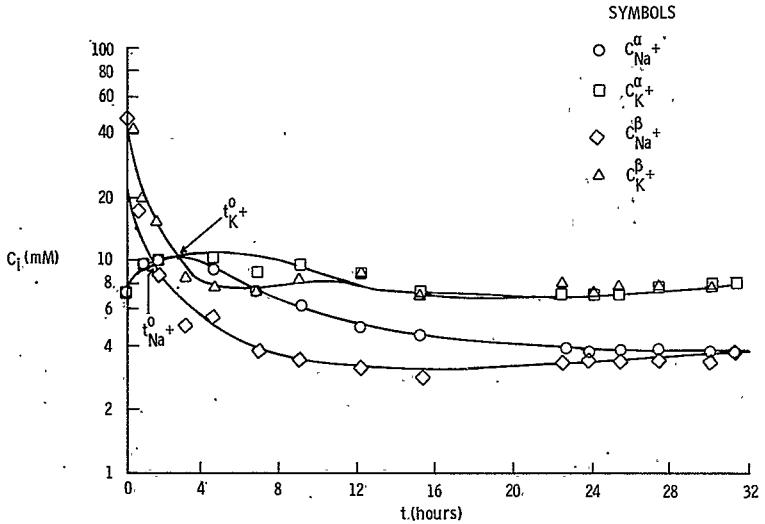
Figure 10.- Experimental variation of Na^+ and K^+ concentrations in compartments α and β with time. $F_w^\gamma = -0.183$ to -0.199 ml/min, temperature = 25.0° C, $C_{Na^+}^\gamma = 0.129$ mM, $C_{K^+}^\gamma = 0.123$ mM. Note decreasing $C_{Na^+}^\alpha$ and $C_{K^+}^\alpha$ after t_i^0 indicating Na^+ and K^+ transport against concentration gradients. Stationary state K^+ concentrations are greater than Na^+ concentrations.

TABLE 5.- VALUES OF DISTRIBUTION FUNCTION

Case	F_w^γ, ml/min	$\dfrac{\ln \dfrac{C_{Na^+}^\gamma + C_{Cl^-}^\gamma}{C_{Na^+}^\beta + C_{Cl^-}^\beta}}{\ln \dfrac{C_{K^+}^\gamma + C_{Cl^-}^\gamma}{C_{K^+}^\beta + C_{Cl^-}^\beta}}$
Theoretical	-0.050	1.20
Theoretical (Fig. 7)	-0.100	1.20
Experiment 10 (Table 3)	-0.075	1.17
Theoretical	-0.159	1.21
Theoretical (Fig. 8)	-0.167	1.20
Experiment 7 (Fig. 10)	-0.190	1.15
Theoretical (Fig. 9)	-0.198	1.20
Experiment 9 (Appendix B)	-0.230	1.19

TABLE 6.- STEADY-STATE EXPERIMENTS; F_w^α, $= - (AL_p \Delta P)^{\alpha\beta} = 0$; $\alpha\beta$ MEMBRANE $\equiv$ MILLIPORE VC; $\beta\gamma$ MEMBRANE $\equiv$ MILLIPORE GS; TEMP. $\equiv 25.0°$ C

Exp. No.	F_w^γ	$c_{Na^+}^{\alpha in}$	$c_{Na^+}^\gamma$	$c_{Na^+}^\gamma/c_{Na^+}^\alpha$	$c_{Na^+}^\beta$	$\Delta J_{Na^+}^\alpha$	$c_{K^+}^{\alpha in}$	$c_{K^+}^\gamma$	$c_{K^+}^\gamma/c_{K^+}^\alpha$	$c_{K^+}^\beta$	$\Delta J_{K^+}^\alpha$
	cc/min	mM	mM		mM	mM/HR	mM	mM		mM	mM/HR
1	0	85.0	102	1.17	92.3	+0.024	85.0	100	1.15	92.0	+0.028
2	-0.073	100	101	1.12	47.4	-0.107	100	100	1.11	54.8	-0.107
3	-0.164	100	101	1.11	25.0	-0.163	100	99.0	1.11	32.0	-0.215
4	-0.263	100	101	1.12	12.1	-0.225	100	100	1.15	17.8	-0.279
5	-0.620	100	103	1.14	6.30	-0.225	100	100	1.14	7.70	-0.290
6	-0.660	100	103	1.14	5.50	-0.225	100	100	1.14	6.60	-0.288
7	-0.670	100	101	1.12	5.40	-0.222	100	100	1.15	6.50	-0.284
8	-0.690	100	101	1.12	5.40	-0.222	100	100	1.15	6.60	-0.284
9	0	40.0	102	2.24	76.7	+0.078	40.0	100	2.11	77.4	+0.108
10	-0.073	49.0	101	2.23	27.5	-0.031	50.8	102	2.18	37.5	-0.034
11	-0.164	50.0	102	2.23	15.4	-0.073	50.7	102	2.27	21.0	-0.095
12	-0.263	50.0	102	2.32	7.04	-0.090	50.5	101	2.41	11.4	-0.120
13	-0.464	50.0	99.3	2.23	3.66	-0.115	50.0	98.0	2.27	4.90	-0.143
14	-0.560	50.0	100	2.23	3.20	-0.106	50.0	100	2.30	4.00	-0.142
15	-0.570	50.0	100	2.23	3.20	-0.103	50.0	100	2.32	4.00	-0.142
16	-0.578	50.0	100	2.23	3.20	-0.102	50.0	100	2.33	4.00	-0.142
17	0	14.5	98.5	4.38	68.3	+0.127	13.8	99.0	4.08	68.8	+0.165
18	-0.118	25.0	99.0	4.23	15.5	-0.015	25.0	98.0	4.00	22.4	-0.005
19	-0.263	25.0	101	5.03	4.80	-0.041	25.0	101	5.15	8.00	-0.045
20	-0.390	25.0	100	4.71	2.10	-0.037	25.0	100	4.92	2.80	-0.046
21	-0.410	25.0	100	4.65	2.10	-0.035	25.0	100	4.85	2.80	-0.045
22	-0.720	10.0	99.0	12.5	0.60	-0.020	10.0	99.0	13.7	0.70	-0.026
23	-0.600	4.95	99.0	24.8	0.56	-0.009	5.00	99.0	25.7	0.61	-0.011

The gradients are given as ranges rather than as specific values because
to have experimentally set them to specific values would have required
a priori knowledge of the data to be determined. The concentrations of
ions in compartment γ were between 98.0 and 102 mM. The membranes
consisted of the Millipore VC type at the $\alpha\beta$ position and the Millipore
GS type at the $\beta\gamma$ position. The dashed lines in the figures represent
analogous theoretical data. Calculations were performed for values of
the empirical parameters $\eta^{\alpha\beta}$ = 0.217, $\eta^{\beta\gamma}$ = 0.585, and θ = 1.6. These
values were obtained by matching two specific theoretical points to the
corresponding experimental points in Figures 11 and 12. These points
were $\Delta J^{\alpha}_{Na^+}$ at F^{γ}_w = -0.7 and $C^{\beta}_{Na^+}$ at F^{γ}_w = -0.3. Both the steady state
analytical and experimental results in Figures 11, 13, and 15 produced
similar plots of ion transport versus water flow across the $\beta\gamma$ membrane
in all cases. Since in all cases studied the concentrations in compart-
ment γ were higher than those in compartment α, ions diffused from
compartment γ to compartment α at zero water flow rate, i.e., ΔJ^{α}_i was
positive. Since the concentrations in α and γ were maintained constant,
diffusion proceeded at a steady-state rate, with K^+ diffusing at a
greater rate than Na^+. The effect of a low water flow across the $\beta\gamma$
membrane, that is, opposing the direction of diffusion, has the effect
of decreasing the rate of diffusion. At a higher F^{γ}_w, the diffusion is
blocked, i.e., ΔJ^{α}_i becomes equal to zero. Na^+ diffusion, since it
proceeds at a lower rate for the same gradient, is blocked at a lower
water flow rate than is K^+ diffusion. At water flows greater than those
causing diffusion blockage of an ion the transport direction of that ion
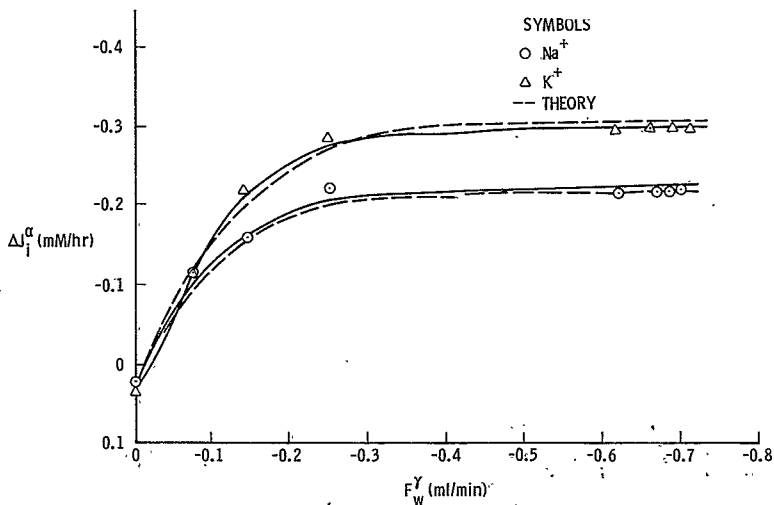
Figure 11.- Variation of Na^+ and K^+ transport with water flow across $\beta\gamma$ membrane; $F_W^\alpha = 0$; $c_i^\gamma/c_i^\alpha = 1.11$ to 1.17; temperature $= 25.0^\circ$ (Theoretical: $\eta^{\alpha\beta} = 0.217$, $\eta^{\beta\gamma} = 0.585$, $\theta = 1.6$, $c_i^\gamma/c_i^\alpha = 1.14$. Note that the greater part of the curves are in the negative ΔJ_i^α region indicating Na^+ and K^+ transport from α to γ against concentration gradients.

Figure 12.- Variation of Na^+ and K^+ concentrations in compartment β with water flow across $\beta\gamma$ membrane; $F_W^\alpha = 0$; $c_i^\gamma/c_i^\alpha = 1.11$ to 1.17; temperature $= 25^\circ$ C. Theoretical: $\eta^{\alpha\beta} = 0.217$, $\eta^{\beta\gamma} = 0.585$, $\theta = 1.6$, $c_i^\gamma/c_i^\alpha = 1.14$. Note that the concentration of K^+ is greater than that of Na^+ within compartment β, the "cellular" compartment.
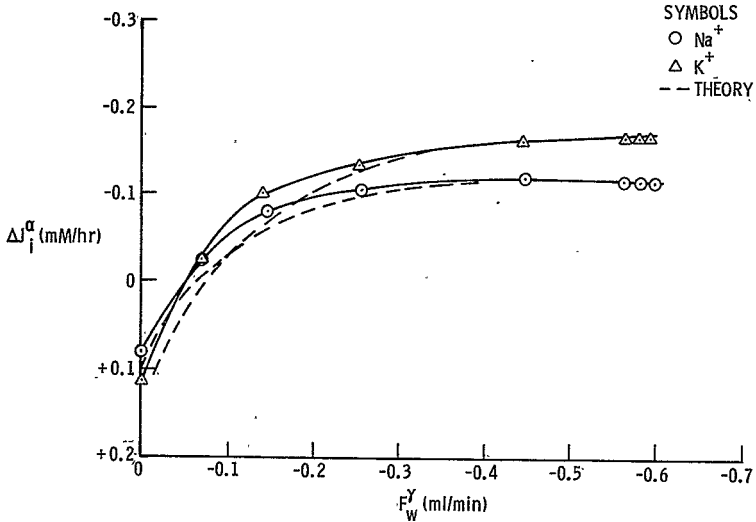
Figure 13.- Variation of Na^+ and K^+ transport with water flow across $\beta\gamma$ membrane; $F_w^\alpha = 0$; $C_i^\gamma/C_i^\alpha = 2.11$ to 2.41; temperature $= 25.0^\circ$ C. Theoretical: $\eta^{\alpha\beta} = 0.217$, $\eta^{\beta\gamma} = 0.585$, $\theta = 1.6$, $C_i^\gamma/C_i^\alpha = 2.2$. Note that the greater part of the curves are in the negative ΔJ_i^α region indicating Na^+ and K^+ transport from α to γ against concentration gradients. Also, note that the transport is less than that against the smaller gradient in Figure 11.
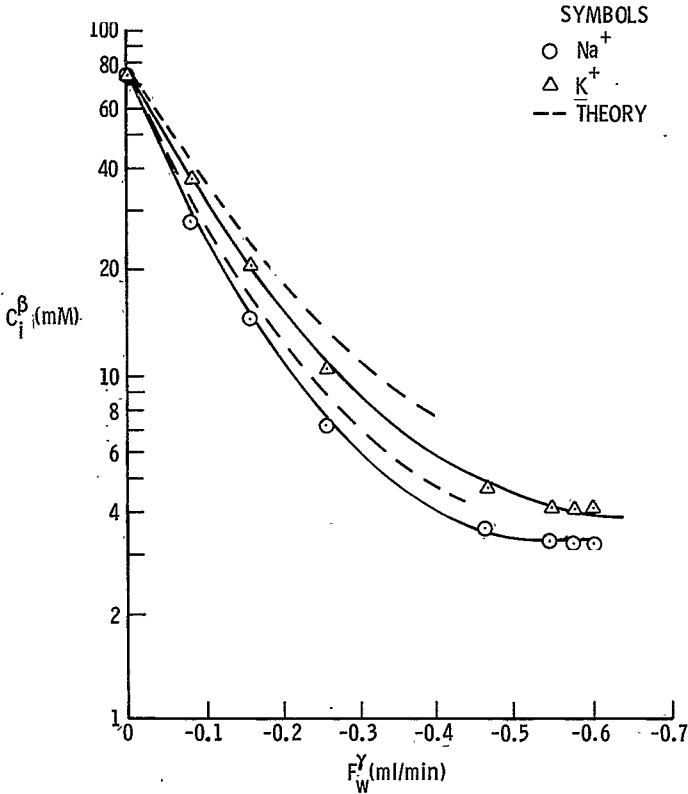
Figure 14.- Variation of Na^+ and K^+ concentrations in compartment β with water flow across $\beta\gamma$ membrane; $F_w^\alpha = 0$; $C_i^\gamma/C_i^\alpha = 2.11$ to 2.41; temperature $= 25.0^\circ$ C. Theoretical: $\eta^{\alpha\beta} = 0.217$, $\eta^{\beta\gamma} = 0.585$, $\theta = 1.6$, $C_i^\gamma/C_i^\alpha = 2.2$. Note that the concentration of K^+ is greater than that of Na^+ within compartment β, the "cellular" compartment. Also note that both Na^+ and K^+ concentrations are lower than those for a smaller ratio C_i^γ/C_i^α in Figure 12.
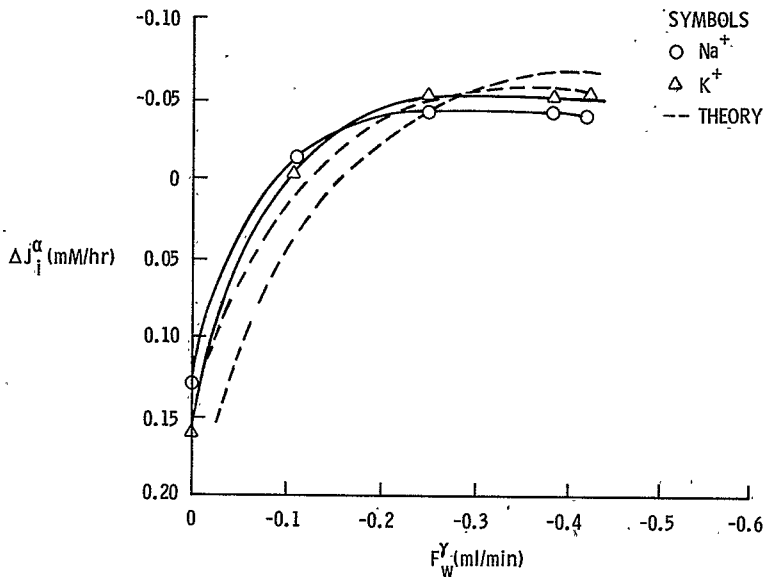
Figure 15.- Variation of Na^+ and K^+ transport with water flow across $\beta\gamma$ membrane; $F_W^\alpha = 0$; $C_i^\gamma/C_i^\alpha = 4.00$ to 5.15; temperature $= 25.0^\circ$ C. Theoretical: $\eta^{\alpha\beta} = 0.217$, $\eta^{\beta\gamma} = 0.585$, $\theta = 1.6$, $C_i^\gamma/C_i^\alpha = 4.5$.

Note that ion transport down concentration gradients, positive ΔJ_i^α, are greater and the transport against concentration gradients, negative ΔJ_i^α, are smaller than transport for smaller gradients in Figures 11 and 13.
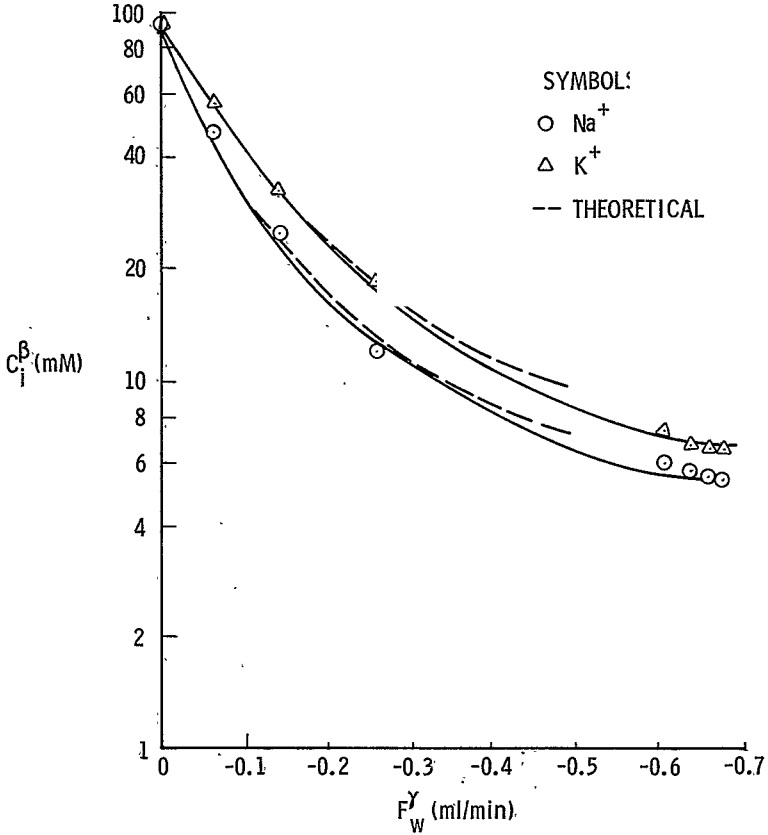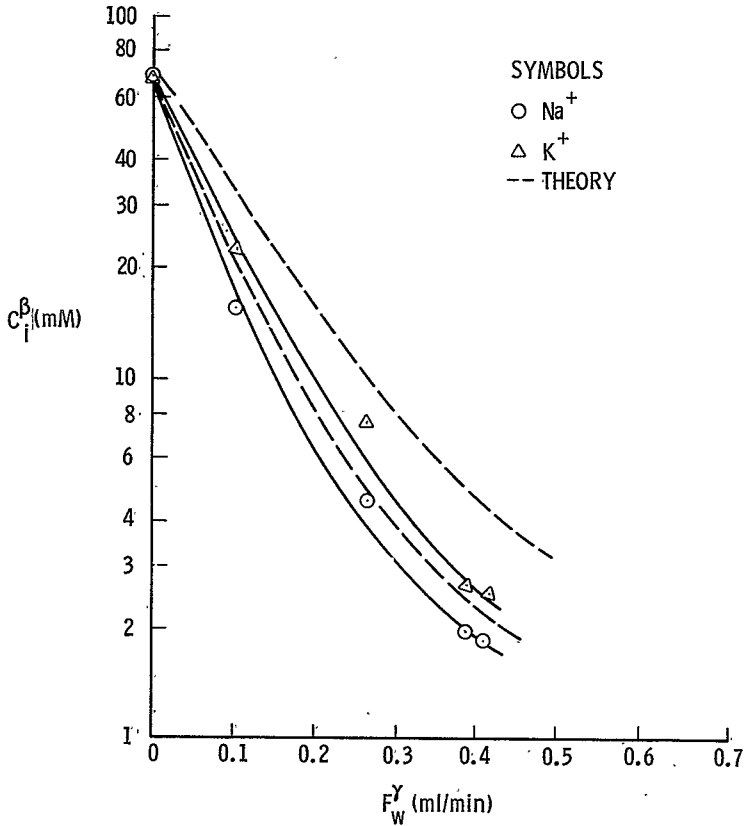
Figure 16.- Variation of Na^+ and K^+ concentrations in compartment β with water flow across $\beta\gamma$ membrane; $F_w^\alpha = 0$; $C_i^\gamma/C_i^\alpha = 4.00$ to 5.15; temperature = 25.0° C. Theoretical: $\eta^{\alpha\beta} = 0.217$, $\eta^{\beta\gamma} = 0.585$, $\theta = 1.6$, $C_i^\gamma/C_i^\alpha = 4.5$. Note that the ion concentrations are lower than those for smaller ratios C_i^γ/C_i^α in Figures 12 and 14.

reverses, i.e., ΔJ_i^α becomes negative, and proceeds against its concen-
tration gradient. In the region $\left|F_W^\gamma\right|(\Delta J_{Na^+}^\alpha = 0)\left| < \left|F_W^\gamma\right| < \left|F_W^\gamma\right|(\Delta J_{K^+}^\alpha = 0)\right.$,
Na^+ and K^+ move in opposite directions even though the concentration
gradient for each is of the same magnitude and sign. At water flow
rates greater than those causing K^+ diffusion blockage, the transport of
both Na^+ and K^+ occurs against their respective concentration gradients.
This transport increases with increasing water flow. This increase in
transport with water flow, however, is at a decreasing rate until at
very high water flow rates the ionic transport is essentially constant.
This constant value is greater for K^+ than for Na^+ because the transport
is proportional to the rate of diffusion across the $\alpha\beta$ membrane. Since
K^+ diffusion is greater than that of Na^+ for the same gradient, the
transport of K^+ is greater. The steady state plots shown in Figures 12,
14, and 16 relate the ion concentrations in compartment β to the water
flow rates. These figures show the continuously decreasing values of
ion concentration with increasing water flow. The concentration of K^+
is higher than that of Na^+, again demonstrating the tendency for K^+ to
remain high within the "cellular" compartment. The results given in
Figures 11-16 also show that as the gradient, C_i^γ/C_i^α, is increased, the
transport down this gradient increases and the transport against this
gradient decreases for the same water flow rate, F_W^γ. The ion concentra-
tions in compartment β also decrease with an increase in this gradient.

Table 7 gives experimental transport data for a range of water flows
across both the $\alpha\beta$ and the $\beta\gamma$ membranes. The results are difficult to
interpret. The experimental errors for these experiments were quite

TABLE 7.- STEADY-STATE EXPERIMENTS, $\alpha\beta$ and $\beta\gamma$ MEMBRANES $\equiv$ MILLIPORE GS;

TEMPERATURE $\equiv 25.0^\circ$ C

Exp. No.	F_w^γ	F_w^α	$C_{Na^+}^{\alpha in}$	$C_{Na^+}^\gamma$	$C_{Na^+}^\gamma/C_{Na^+}^\alpha$	$C_{Na^+}^\beta$	$\Delta J_{Na^+}^\alpha$	$C_{K^+}^{\alpha in}$	$C_{K^+}^\gamma$	$C_{K^+}^\gamma/C_{K^+}^\alpha$	$C_{K^+}^\beta$	$\Delta J_{K^+}^\alpha$
	cc/min	cc/min	mM	mM		mM	mM/HR	mM	mM		mM	mM/HR
24	-0.135	0	100	100	1.12	32.8	-0.145	100	100	1.15	40.1	-0.157
25	-0.252	0	100	100	1.13	18.5	-0.185	100	100	1.18	22.8	-0.231
26	0	+0.091	120	100	1.04	42.5	+0.156	120	100	1.03	51.0	+0.175
27	-0.135	+0.100	140	100	1.10	14.6	-0.040	140	100	1.10	23.3	-0.040
28	-0.252	+0.103	140	100	1.08	8.05	-0.049	140	100	1.10	9.90	-0.084
29	-0.437	+0.150	140	100	1.09	1.41	-0.013	140	100	1.10	2.64	-0.038

large due to difficulties in controlling and measuring three different

flows simultaneously: F_w^γ, F_w^α, and $F_{saline}^{\alpha\ in}$. However, the data do

indicate that the ion transport in the positive direction increases and

ion transport in the negative direction decreases with increasing water

flow across the $\alpha\beta$ membrane, i.e., when $F_w^\alpha > 0$. This was also demon-

strated with theoretical data as shown in Figure 18. These data also

demonstrate that the relative values of $\eta^{\alpha\beta}$ and $\eta^{\beta\gamma}$ are very useful in

determining the degree to which the transport is increased or decreased.

As shown in Figure 18, for a ratio of $\eta^{\beta\gamma}/\eta^{\alpha\beta}$ equal to 2.7, transport in

the negative direction is almost totally blocked for all values of water

flow across the $\beta\gamma$ membrane by a flow across the $\alpha\beta$ membrane equal to

+.1 ml/min. Furthermore, in comparing Figures 12 and 17 it may be seen

that for the same total water flow into the system, $|F_w^\alpha|+|F_w^\gamma|$, the ior

concentrations in compartment β are lower if part of the water flow

occurs across the $\alpha\beta$ membrane. An increase in water flow, F_w^α, across

the $\alpha\beta$ membrane causes an increased differentiation between Na^+ and K^+

transport over most of the water flow range, F_w^γ. These theoretical data

are shown in Table 8.

In view of the significance of the membrane parameters $\eta^{\alpha\beta}$ and $\eta^{\beta\gamma}$,

on the theoretical results, an analysis was performed to determine the

effects of variation of these parameters for the $\alpha\beta$ and $\beta\gamma$ membranes on

transport rates and on the ion concentrations in compartment β. At zero

water flow across the $\alpha\beta$ membrane, the transport proceeds at the rate of

diffusion across that membrane. A decrease in $\eta^{\alpha\beta}$, which means a

decrease in diffusion area or decrease in gradient, produces a decrease
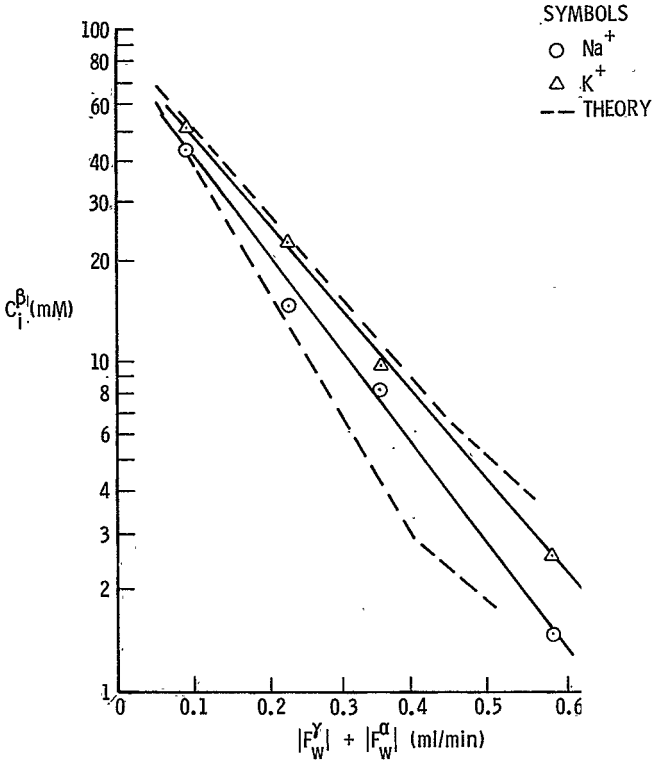
Figure 17.- Variation of Na^+ and K^+ concentrations in compartment β with water flow across membranes $\alpha\beta$ and $\beta\gamma$; $F_W^\alpha = 0.091$ to 0.150 ml/min; $c_i^\gamma/c_i^\alpha = 1.03$ to 1.10; temperature = 25.0° C. Theoretical: $\eta^{\alpha\beta} = 0.217$, $\eta^{\beta\gamma} = 0.585$, $\theta = 1.6$, $c_i^\gamma/c_i^\alpha = 1.14$, $F_W^\alpha = 0.1$ ml/min. Note that the ion concentrations in compartment β are much lower than those for the same ratio c_i^γ/c_i^α and same total water flow in Figure 14. This is due to diffusion blockage by the water flow across the $\alpha\beta$ membrane.
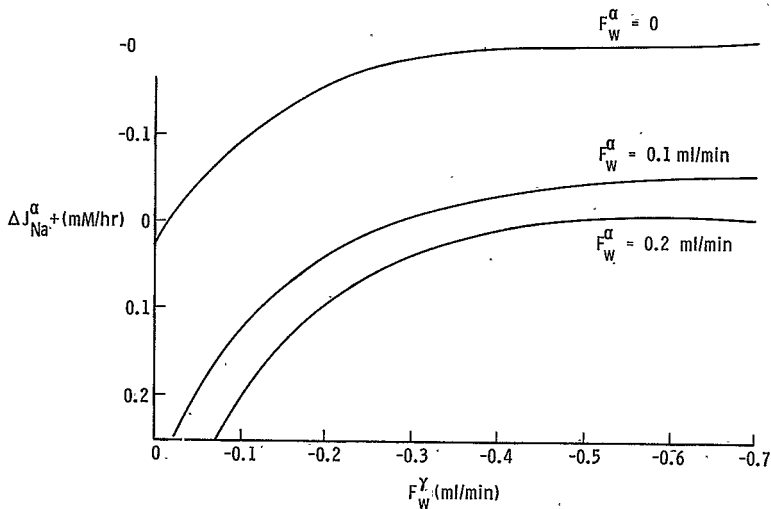
Figure 18. - Theoretical variation of Na^+ transport with water flow across $\beta\gamma$ membrane and water flow across $\alpha\beta$ membrane.

$C^\gamma_{Na^+}/C_{Na^+} = 1.14$, $\eta^{\alpha\beta} = 0.217$, $\eta^{\beta\gamma} = 0.585$. Note that for the values of η employed transport against the concentration gradient, negative ΔJ^α_1, is almost totally blocked for all values of F^γ_w by a water flow across the $\alpha\beta$ membrane equal to 0.1 ml/min.

TABLE 8.- THEORETICAL VARIATION OF RATIO OF K^+ TO Na^+ TRANSPORT WITH TOTAL WATER

FLOW FOR THREE RATES OF FLOW ACROSS THE $\alpha\beta$ MEMBRANE

F_w^{Tot}	F_w^{α}	F_w^{γ}	$\Delta J_{K^+}^{\alpha}/\Delta J_{Na^+}^{\alpha}$	F_w^{α}	F_w^{γ}	$\Delta J_{K^+}^{\alpha}/\Delta J_{Na^+}^{\alpha}$	F_w^{α}	F_w^{γ}	$\Delta J_{K^+}^{\alpha}/\Delta J_{Na^+}^{\alpha}$
0	0	0	1.05	0.10	--	--	0.20	--	--
0.05	0	-0.05	1.04	0.10	--	--	0.20	--	--
0.10	0	-0.10	1.11	0.10	0	1.16	0.20	--	--
0.15	0	-0.15	1.16	0.10	-0.05	1.25	0.20	--	--
0.20	0	-0.20	1.22	0.10	-0.10	1.35	0.20	0	1.24
0.25	0	-0.25	1.25	0.10	-0.15	1.49	0.20	-0.05	1.35
0.30	0	-0.30	1.29	0.10	-0.20	1.62	0.20	-0.10	1.47
0.35	0	-0.35	--	0.10	-0.25	1.92	0.20	-0.15	1.60
0.40	0	-0.40	1.35	0.10	-0.30	0.938	0.20	-0.20	1.76
0.45	0	-0.45	--	0.10	-0.35	--	0.20	-0.25	1.95
0.50	0	-0.50	1.38	0.10	-0.40	1.76	0.20	-0.30	2.12
0.60	0	-0.60	1.41	0.10	-0.50	1.92	0.20	-0.40	2.52
0.70	0	-0.70	1.44	0.10	-0.60	2.04	0.20	-0.50	3.21
0.80	0	-0.80	--	0.10	-0.70	2.13	0.20	-0.60	2.55
0.90	0	-0.90	--	0.10	-0.80	--	0.20	-0.70	3.25

in transport for all values of water flow across the $\beta\gamma$ membrane. This is shown in Figures 19 and 20. Decreasing $\eta^{\alpha\beta}$, and thereby decreasing diffusion into compartment β, has the effect of decreasing ion concentrations in β for the same water flow. This is shown in Figure 21. A decrease in $\eta^{\beta\gamma}$, or, in effect, a decrease in effective pore area or in gradient for the $\beta\gamma$ membrane, results in an increase in ion transport in the direction of water flow. This occurs because of an increase in water flux, a reduced gradient against which transport takes place, and decreased back diffusion. This case is shown in Figures 22 and 23. As shown in Figure 24, a decrease in $\eta^{\beta\gamma}$ reduces ion concentrations in compartment β. Again, this occurs because of a reduced back diffusion across the $\beta\gamma$ membrane.

The actual biological problem is much more complex than the model presented in this study. However, the basic features of the model consisting of multiple compartments separated by phase boundaries with material flows across them exist in all biological systems. The phenomena which occur in such a model must also occur in a biological system since both are governed by the same physical laws. Although the flows of material across a cell membrane may be small, the transport phenomena, as presented here, are a function of the velocities of the components. These velocities may be extremely large due to the small pore areas thought to exist in the living membrane. The flow of water considered in this study is only one of many metabolic component flows which traverse the living cell membrane. Components other than water may be more efficient in transporting ions. Flows of glucose, lactic

Figure 19.- Theoretical variation of Na^+ transport with water flow across the $\beta\gamma$ membrane and $\eta^{\alpha\beta}$. $C^{\gamma}_{Na^+}/C^{\alpha}_{Na^+} = 1.14$, $\eta^{\beta\gamma} = 1.0$. Note increase in negative transport with increase in area or decrease in thickness of the $\alpha\beta$ membrane.
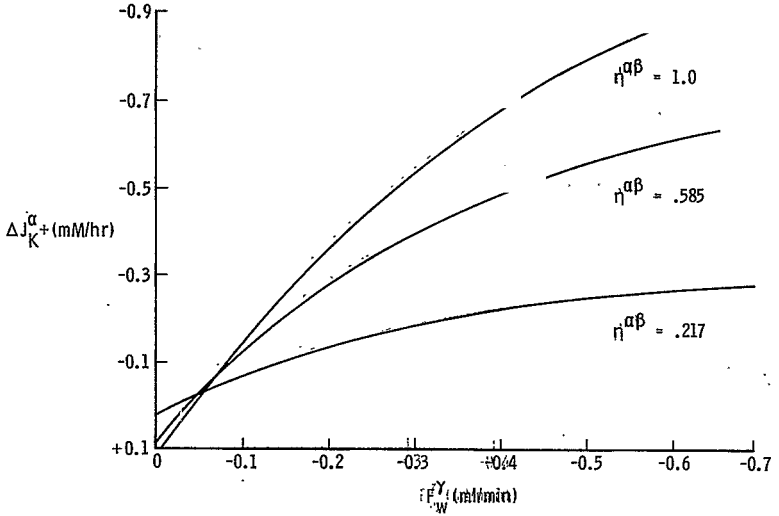
Figure 20.- Theoretical variation of K^+ transport with water flow across $\beta\gamma$ membrane and $\eta^{\alpha\beta}$. $c_K^\gamma/c_K^\alpha = 1.14$, $\eta^{\beta\gamma} = 1.0$. Note increase in negative transport with increase in area or decrease in thickness of the $\alpha\beta$ membrane.
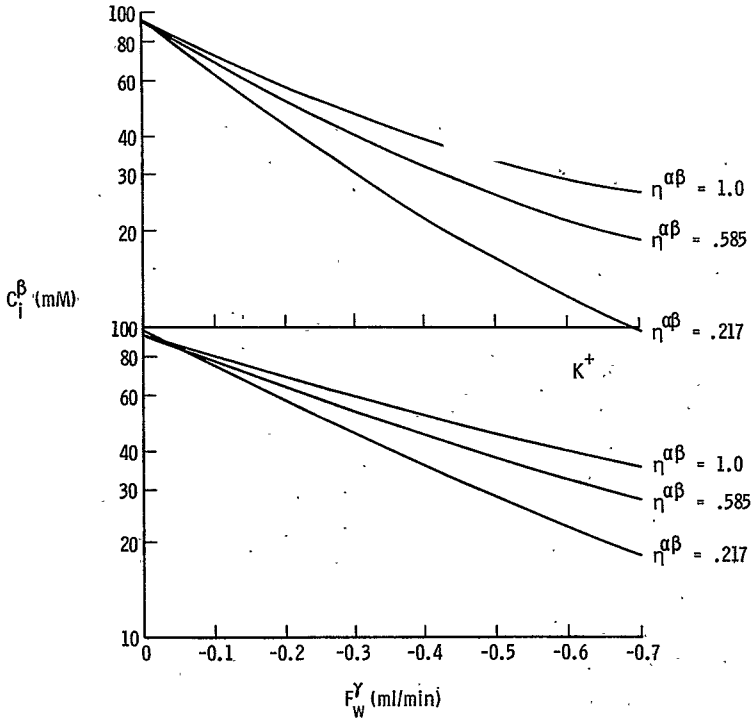
Figure 21.- Theoretical variation of Na^+ and K^+ concentrations in compartment β with water flow across the $\beta\gamma$ membrane and $\eta^{\alpha\beta}$. $c_i^\gamma/c_i^\alpha = 1.14$, $\eta^{\beta\gamma} = 1.0$. Note increase in Na^+ and K^+ concentrations in compartment β with increase in area or decrease in thickness of the $\alpha\beta$ membrane.
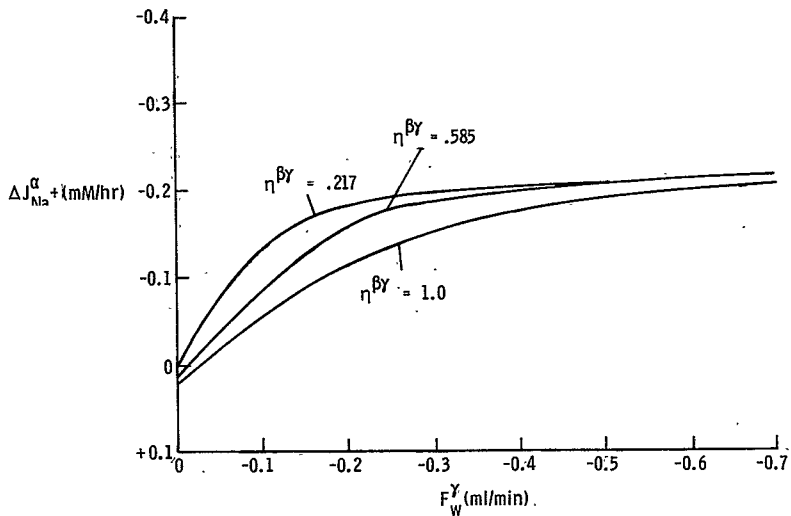
Figure 22.- Theoretical variation of Na^+ transport with water flow across the $\beta\gamma$ membrane and $\eta^{\beta\gamma}$. $C_{Na^+}^\gamma/C_{Na^+}^\alpha = 1.14$, $\eta^{\alpha\beta} = 0.217$.

Note increase in transport rates with decrease in area or increase in thickness of the $\beta\gamma$ membrane.
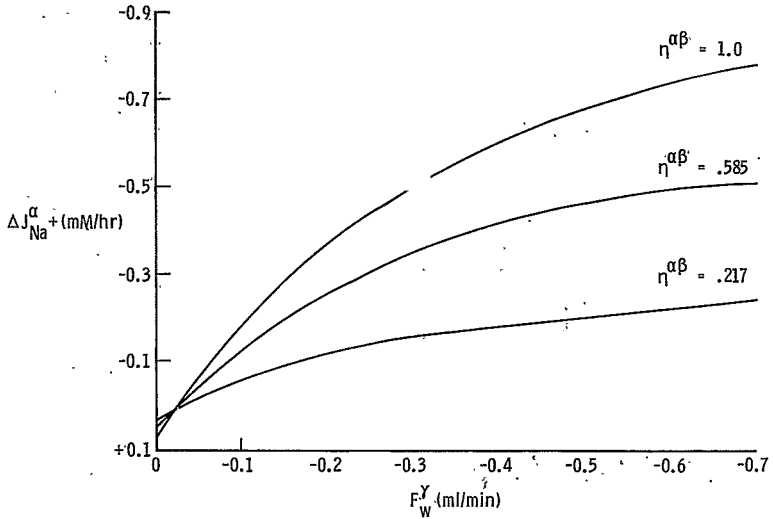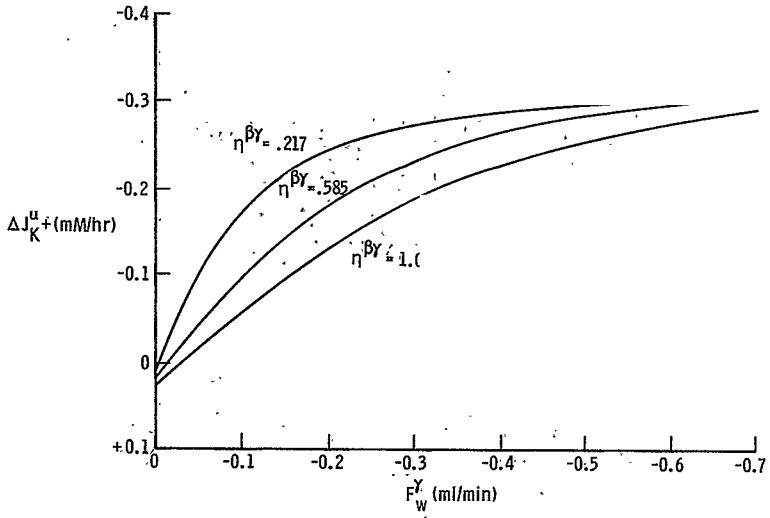
Figure 23.- Theoretical variation of K^+ transport with water flow across $\beta\gamma$ membrane and $\eta^{\beta\gamma}$. $C_{K^+}^{\gamma}/C_{K^+}^{\alpha} = 1.14$, $\eta^{\alpha\beta} = 0.217$.

Note increase in transport rates with decrease in area or increase in thickness of the $\beta\gamma$ membrane.
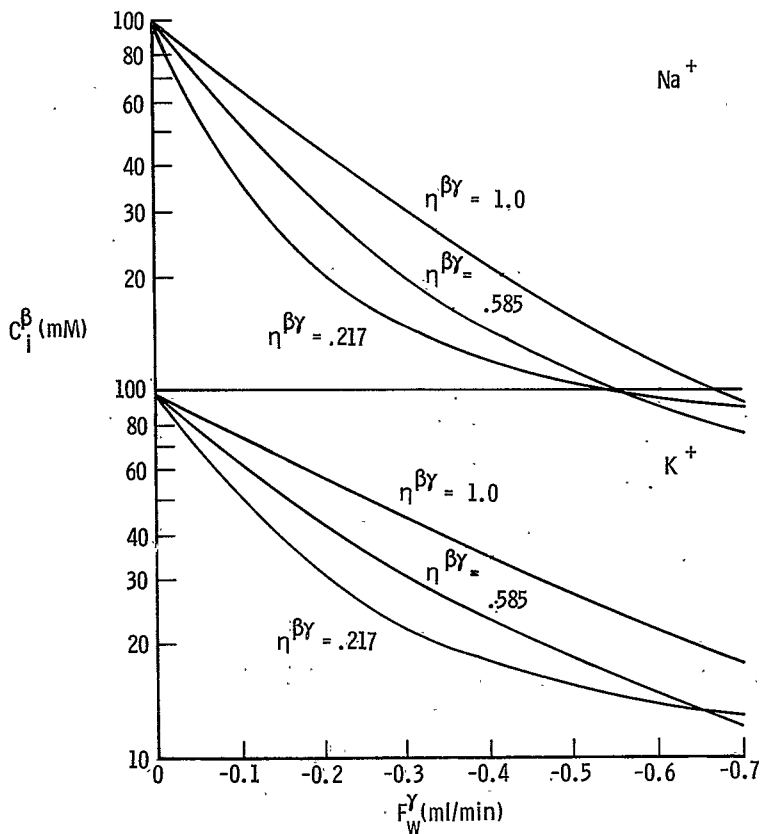
Figure 24.- Theoretical variation of Na^+ and K^+ concentrations in compartment β with flow of water across $\beta\gamma$ membrane and $\eta^{\beta\gamma}$. $C_i^\gamma/C_i^\alpha = 1.14$, $\eta^{\alpha\beta} = 0.217$. Note decrease in Na^+ and K^+ concentrations in compartment β with decrease in area or increase of the $\beta\gamma$ membrane.

acid, urea, ammonia, and carbon dioxide have been shown to be able to transport ions (27,38).

The membranes utilized in this study are simple relative to the biological membranes. Pore sizes in cell membranes, of the order of magnitude of hydrated ions, would have the effect of increasing the tendency to differentiate between ions. The ions having greater permeability would tend to move in an opposite direction to the transport of ions of lesser permeability in order to maintain electroneutrality across the cell membrane.

An analogy may be made between the model of this study and a three-compartment biological system such as the kidney (13, 23, 30, 34). In general, Na^+ ions are thought to move from the kidney tubule lumen into the tubule cell down a concentration gradient existing across the lumenal membrane. The Na^+ is then transported out of the cell compartment into the interstitial fluid compartment against a concentration gradient existing across the basal membrane. This is consistent with the model if it is assumed that the fluxes of components essential to the transport mechanism are greater between the cell and the interstitial compartment than between the cell and the lumen compartment. An indication that this indeed may be so in the proximal tubule is the fact that the mitochondria in the proximal tubule cells are primarily located within the invaginations of the basal membrane. The model situation in which no water flow exists across the $\alpha\beta$ membrane is analogous to the ascending loop of Henle where it is proposed that Na^+ is transported against a gradient from the lumen to the interstitial fluid while no water moves

between these compartments. The water flow probably is blocked by the lumenal membrane. Other sections of the kidney tubule are variably permeable to water, and thus a water flow may exist across both membranes. As demonstrated by the model, the distribution of flows across the two membranes is dependent on the properties of these two membranes. The brush border on the lumenal side of the proximal tubule cells, for example, could function to greatly increase the pore area of the lumenal membrane relative to the basal membrane and thereby control the magnitude, direction, and differentiation of transport of different ions. This is supported by the data in Figures 19 and 22, which show that in order to maximize Na^+ reabsorption the lumenal membrane should be as large as possible relative to the basal membrane.

CONCLUSIONS

In a two-membrane, three-compartment system in which the concen-
trations of Na^+ and K^+ in the "interstitial" compartment are held
constant, a transient transport of Na^+ and K^+ from the "lumen"
compartment to the "interstitial" compartment against a concentration
gradient may be maintained by a flow of water from the "cell"
compartment to the "interstitial fluid" compartment. This transport
will proceed at a steady-state rate if the Na^+ and K^+ concentrations
in the "lumen" compartment are also held constant.

If the water flow is decreased, the system will reach a point
where the water flow no longer sustains K^+ transport against its
concentration gradient, and the transport of the Na^+ and K^+ will proceed
in opposite directions, K^+ moving down the gradient and Na^+ moving
against an equal or larger gradient. A similar steady-state phenomenon
is observed when concentrations in both the "lumen" and "interstitial
fluid" compartments are held constant.

For the same water flow across the membrane separating the
"cellular" and "interstitial" compartments, the steady-state Na^+ and K^+
transport against the concentration gradient decreases with increase
of the gradient.

For equal concentrations of Na^+ and K^+ in the "lumen" and "inter-
stitial" compartments, the concentration of K^+ is greater than that
of Na^+ in the "cellular" compartment for all except extremely low

values of water flow from the "cellular" compartment to the "interstitial" compartment.

Both the analytical model and the experiments should be expanded to include membranes which have specific permeabilities for the ions under consideration. They should also be expanded to include nonionic components such as glucose and urea.

BIBLIOGRAPHY·

1. Binder, R. C.: Fluid Mechanics. rrenтice-наιι, 1962, 114-116.

2. Brown, A. C.: Passive and active transport. 'In: Physiology and Biophysics, edited by Ruch and Patton. 19th ed. Saunders, 1965, . 820-842.

3. Catalog MF-67. Millipore Corporation, Bedford, Massachussets, 1967.

4. Davies, P. W.: Membrane theory and resting potential. In: Medical Physiology, edited by P. Bard. 11th ed., C. V. Mosby, 1961, 934-945.

5. Davson, H.: A Textbook of General Physiology. Little, Brown, and Co., 1959, 1-490.

6. Denbigh, K. G.: The Thermodynamics of the Steady State. London: Methuen, 1951, 103 p.

7. Dunlop, P. J.; and L. J. Gosting: Use of diffusion and thermodynamic data to test the Onsager reciprocal relation for isothermal diffusion in the system NaCl-KCl-H_2O at 25°. J. Phys. Chem. 63:86-93, 1959.

8. Ekman, A.; J. Rastas; and S. Salminen: 'Stationary distribution of ions across a membrane in the system sodium chloride-potassium chloride-hydrochloric acid-water. Nature. 200:1070-1073, 1963.

9. Fitts, D. D.: Non-equilibrium Thermodynamics. New York: McGraw-Hill, 1962, 173 p.

10. Fujita, H.; and L. J. Gosting: A new procedure for calculating the diffusion coefficients of three-component systems from Goy diffusiometer data. J. Phys. Chem. 64:1256-1263, 1960.

11. Ganong, W. F.: Review of Medical Physiology. 3rd. ed., Lange, 1967, 621 p.

12. Giese, A. C.: ·Cell Physiology. 2nd ed., Saunders, 1962, 592 p.

13. Gregerson, M. I.: Kidney. In: Medical Physiology. 11th ed., C. V. Mosby, 1961, 332-361.

14. de Groot, S. R.: Thermodynamics of Irreversible Processes. Amsterdam: North-Holland, 1952, 242 p.

15. de Groot, S. R.; and P. Mazur: Non-Equilibrium Thermodynamics. New York: Interscience, 1962, 510 p.

16. Haase, R.: Thermodynamik der Irreversiblen Prozesse. Darmstadt: Steinkopf, 1963, 552 p.

17. Harned, H. S.; and B. B. Owen: The Physical Chemistry of Electrolytic Solutions. New York: Reinhold, 1958.

18. Hearon, J. Z.: Some cellular diffusion problems based on Onsager's generalization of Fick's law. Bull. Math. Biophys. 12:135-159, 1950.

19. Katchalsky, A.; and P. F. Curran: Nonequilibrium Thermodynamics in Biophysics. Harvard, 1965, 248 p.

20. Katz, A. I.; and F. H. Epstein: Physiologic role of sodium-potassium-activated adenosine triphosphatase in the transport of cations across biologic membranes. N. England J. Med., 278:253-261, 1968.

21. Kedem, O.; and A. Katchalsky: Thermodynamic analysis of the permeability of biological membranes to non-electrolytes. Biochem. Biophys. Acta., 27:229-246, 1958.

22. Kedem, O.; and A. Katchalsky: A physical interpretation of the Phenomenalogical coefficients of membrane permeability. J. Gen. Physiol., 45:143-179, 1961.

23. Koch, A.: The Kidney. In: Physiology and Biophysics, edited by Ruch and Patton. 19th ed., Saunders, 1965, 843-870.

24. Manning, G. S.: Binary diffusion and bulk flow through a potential energy profile: A kinetic basis for the thermodynamic equations of flow through membranes. J. Chem. Phys., 40:2668-2675, 1968.

25. Nims, L. F.: Steady state material transfer through biological barriers. Am. J. Physiol., 201:987-994, 1961.

26. Nims, L. F.; and R. E. Thurber: Ion distribution patterns in stationary state systems. Am. J. Physiol., 201:995-998, 1961.

27. Nims, L. F.; and R. Butera. Ion distribution patterns, membranes and enzymes. Physiologist, 7:216, 1964.

28. Onsager, L.: Reciprocal relations in irreversible processes. I. Phys. Review, 37:2265-2279, 1931; Reciprocal relations in irreversible processes. II. Phys. Review, 38:405-426, 1931.

29. Onsager, L.: Theories and problems of liquid diffusion. _Ann. N. Y._
    Acad. Sci., 46:241-265, 1945.

30. Pitts, R. F.: _Physiology of the Kidney and Body Fluids._ Year Book
    Medical Publishers, 1968, 266 p.

31. Prigogine, I.: _Introduction to Thermodynamics of Irreversible_
    Processes. New York: Interscience, 1968, 147 p.

32. Rapoport, S. I.: Ionic accumulation by water flow through a
    membrane. _Acta Physiol. Scand._, 64:361-371, 1965.

33. Salminen, S.: Transport of ions across membranes. _Nature,_
    200:1069-1070, 1963.

34. Smith, H. W.: _The Kidney._ New York: Oxford University Press,
    1951, 1049 p.

35. Sokolnikoff, I. S.; and R. M. Redheffer: _Mathematics of Physics_
    and Modern Engineering. McGraw-Hill, 1958, 100-106.

36. Spiegler, K. S.: Transport process in ionic membranes. _Trans._
    Faraday Soc., 54:1408-1428, 1958.

37. Stavermann, A. J.: Non-equilibrium thermodynamics of membrane
    processes. _Trans. Faraday Soc._, 48:176-185, 1952.

38. Thurber, R. E.; and A. M. Thompson: Stationary state sodium and
    potassium ion distributions of human erythrocytes. _Am. J._
    Physiol., 212:877-883, 1967.

39. Ussing, H. H.: The frog skin potential. _J. Gen. Physiol._,
    43:135-147, 1959. The distinction by means of tracers between
    active transport and diffusion. _Acta Physiol. Scand._ 19:43-56,
    1949.

40. Van Rysselberghe, P.: _Thermodynamics of Irreversible Processes._
    New York: Blaisdell, 1963, 165 p.

41. Whittam, R.; and K. P. Wheeler: Transport across cell membranes.
    Annual Rev. Physiol. 32:21-60, 1970.

42. 1967 Gelman Catalog. Gelman Instrument Co., Ann Arbor, Michigan.

APPENDIX A

Experimental Apparatus Details

Drawings showing the details of the experimental apparatus are

given in Figures 25-31. Dimensions are given in inches. Descriptions

of the part numbers in the drawings are given in Table 9. The apparatus,

except where indicated otherwise, was made of Lucite.

Because of instability the specific ion electrodes, part No. 46,

were not used as shown. Instead samples were taken and analyzed by

a Beckman atomic absorption system.

The use of a nonwettable membrane for creating an osmotic water

flow is an innovation resulting from this study. This type of membrane

is normally used for filtering organic solvents or passing a gas into

aqueous solutions. Since the membrane will pass water vapor but not

aqueous solution at normal pressures, water may be transferred across

the membrane as a result of a water partial pressure gradient. This

gradient may be established by a difference in the colligative

properties of the solutions on either side of the membrane or a temper-

ature differential. The transfer rate is independent of the pressure

differential across the membrane over a large pressure range. If air

saturation of the membrane is maintained, the water transfer against

a pressure differential is limited only by the burst pressure of the

membrane. Transfer of water against a pressure differential of 20 psi

have been observed.

Some breakthrough of the more viscous saturated LiCl and $CaCl_2$ was observed at membrane support points. This resulted in a decrease in water transfer rate over a period of days. This breakthrough was not observed for the saturated NaCl solutions.
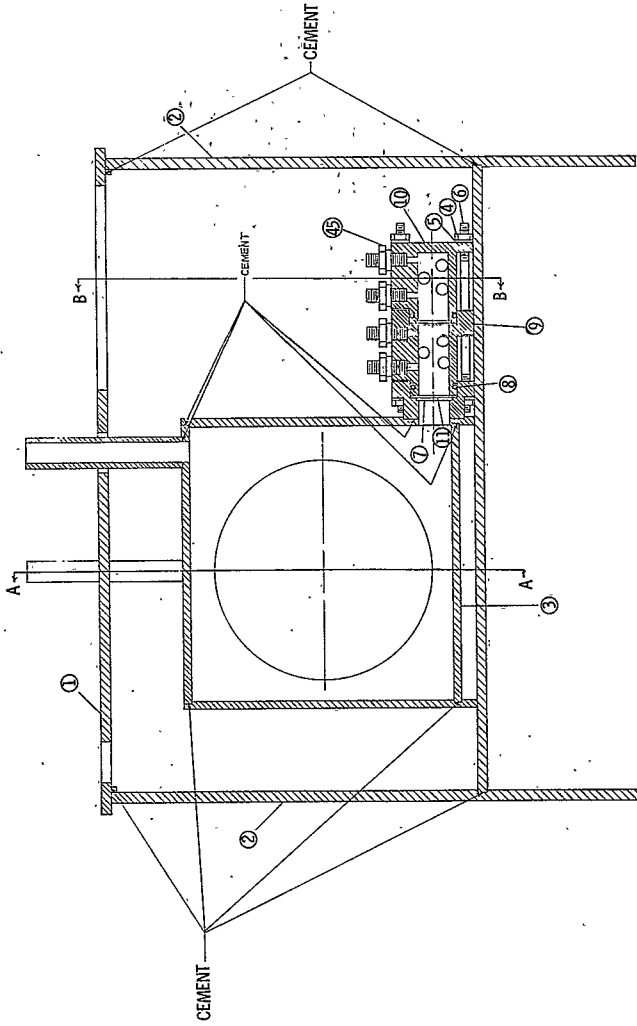
Figure 25.- Apparatus Cross Section
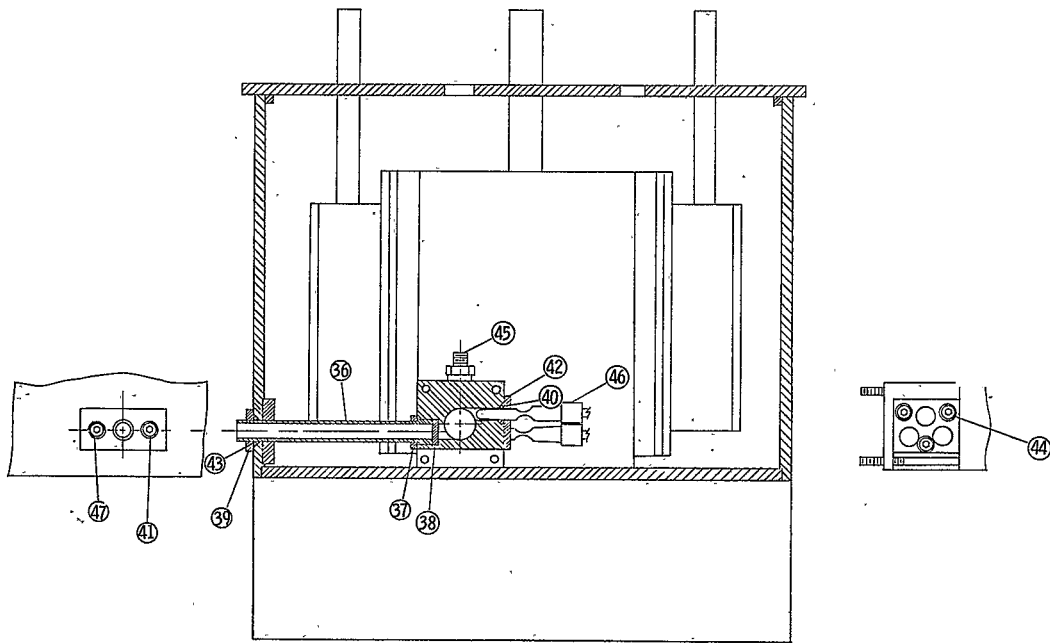
Figure 26.- Cross section through compartment α or β showing sampling port
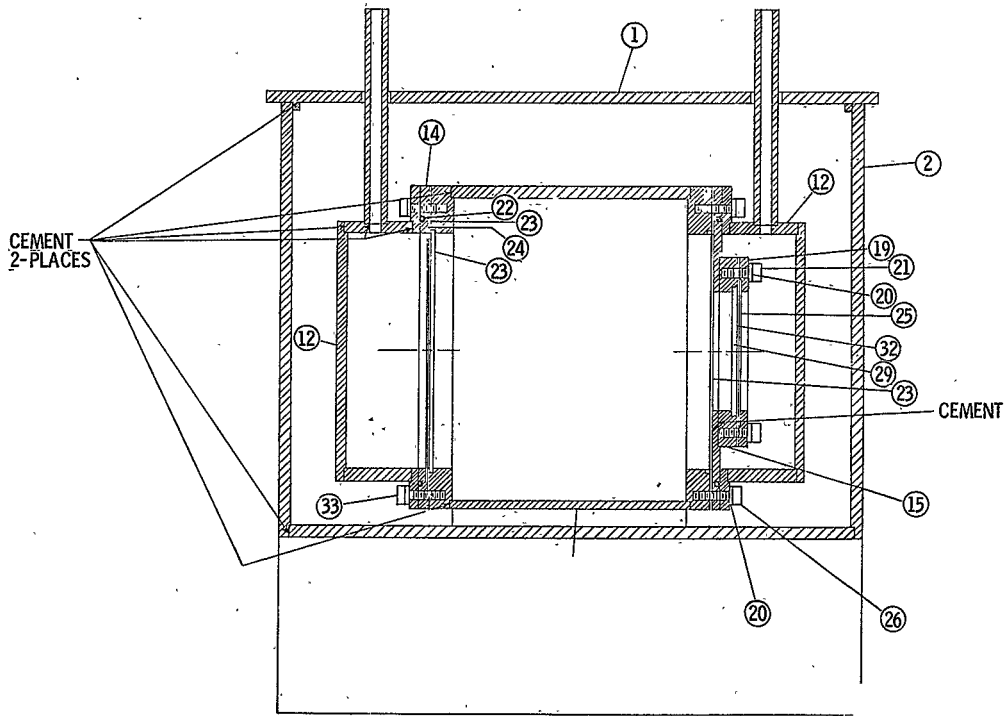
Figure 27.- Cross section of compartment γ and osmotic compartment

Figure 28.— Compartment γ detail.

.250 DIA. HOLE
DRILL 1.00 DEEP
TO INTERSECT .75 BORE
90° COUNTERSINK
TO MAKE .55 O.D.
THREE PLACES

TAP FOR 10-24
3/8 DEEP
HELICOIL INSERT
3 PLACES

13/64 DIA. HOLE
DRILL THROUGH
4 HOLES EQUALLY SPACED
ON 2.150 BCD

1/4 DIA. HOLE DRILL
THROUGH TO .75 BORE,
1.00 DEEP
2 PLACES

TAP FOR 7/16-20 STRAIGHT THREAD
.406 DEEP 2 PLACES

SECTION B-B

3/8 HOLE DRILL
THROUGH TO .75 BORE

.625 + .001 / .000 DIA. HOLE
FLAT BOTTOM
.500 DEEP

TAP FOR 10-24 3/8 DEEP
HELICOIL INSERT
2 PLACES

SECTION A-A

Figure 29.- Compartment β detail.

Figure 30.- Compartment α detail.

CEMENT

CEMENT

.25

4.63   1.75

B-B

15.75

A

CEMENT
2 PLACES

B

COUNTERSINK 90°
to .80 O.D.

A

TAP
FOR 10-24,
.50 DEEP
HELICOIL INSERT

.516
DIA.

.516
DIA.

.80
DIA.

.595

.595

.595

.595

45°

1.850   3.000

B-B 1/1 SCALE

12.50

.25   .25

13.00

.25

3.75

CEMENT

A-A

.75

1.50

.813   .12

A-A 1/1 SCALE

66
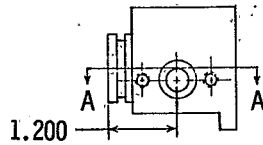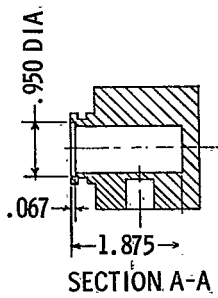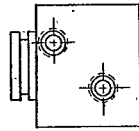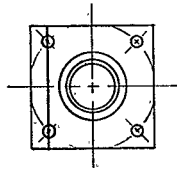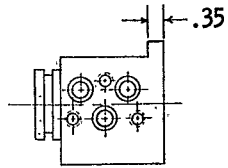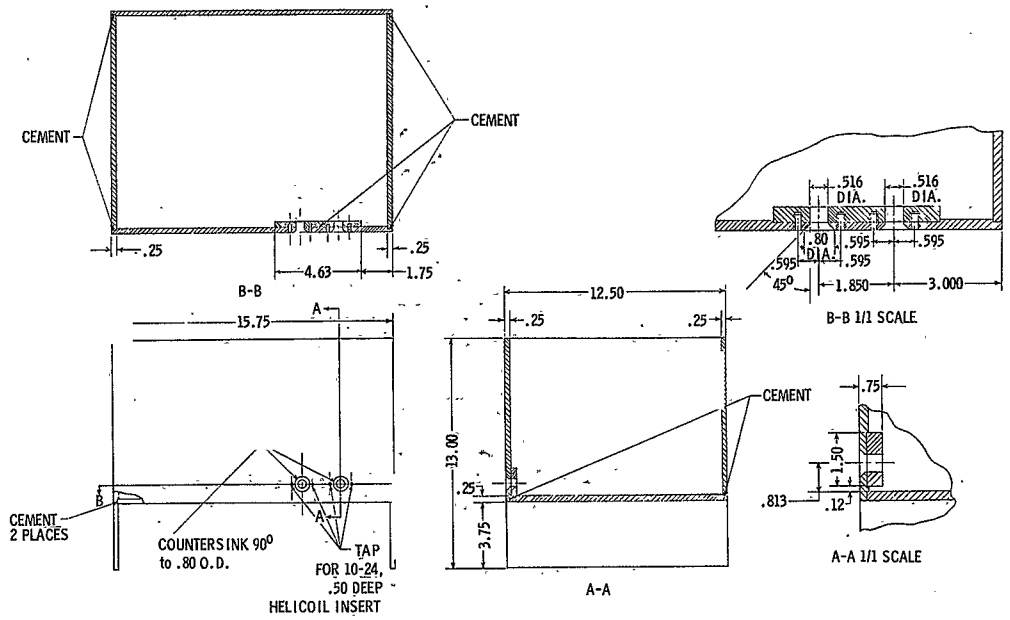
Figure 31.- Water bath detail.

TABLE 9.- EXPERIMENTAL APPARATUS PARTS DESCRIPTION

Part No.	Description
2	Water bath lid
3	Compartment γ
4	Stainless steel nut
5	Stainless steel washer
6	Stainless steel threaded rod
7	Monel screen membrane support
8	Rubber O-ring
9	Compartment β
10	Compartment α
11	Millipore membrane, VC or GS
12, 13	Osmotic compartments
14	Nonwettable membrane retaining ring
15, 16, 18, 19	Spacer disc
20	Stainless steel washer
21	Stainless steel screw
22	Rubber O-ring
23	Rubber gasket
24, 25	Gelman VF-6 membrane
26	Stainless steel screw
27	Stainless steel helicoil inserts
28, 29, 30	Monel screen membrane support
31, 32	Rubber gasket
33	Stainless steel screw
36	Sampling port
37	Stainless steel retaining plate
38	Rubber septum
39	Stainless steel retaining plate
40	Rubber O-ring
41	Stainless steel bolt
42	Stainless steel retaining plate
43	Rubber O-ring
44	Stainless steel bolt
45	Swagelok fitting
46	Specific ion electrode
47	Stainless steel washer

APPENDIX B

Additional Data and Calculated Values

Tables 10 and 11 show the results of nonsteady-state experiments at two additional water flow rates, F_w^γ. The results are similar to those presented in Table 4.

Table 12 shows the concentrations of solution flowing into and out of compartment α, and the time for collecting a 10 ml sample out of compartment α, from which the ion transport rates for the steady-state experiments were calculated.

TABLE 10.- NONSTEADY-STATE EXPERIMENT (NO. 9); $\alpha\beta$ MEMBRANE $\equiv$ GELMAN GA-9,

$\beta\gamma$ MEMBRANE $\equiv$ MILLIPORE GS

$$C_{Na^+}^{\gamma} = 144 \text{ mM}, \quad C_{K^+}^{\gamma} = 160 \text{ mM}, \quad C_{Cl^-}^{\gamma} = 304 \text{ mM}$$

t	F_w^{γ}	Temp.	$C_{Na^+}^{\alpha}$	$C_{Na^+}^{\beta}$	$C_{K^+}^{\alpha}$	$C_{K^+}^{\beta}$	$C_{Cl^-}^{\alpha}$	$C_{Cl^-}^{\beta}$
Hours	ml/min	°C	mM	mM	mM	mM	mM	mM
0	0	--	4.40	29.9	4.90	32.8	9.3	62.7
1	-0.245	24.9	6.20	9.40	7.70	12.1	13.9	21.5
2	-0.258	25.2	5.80	3.60	7.70	6.60	13.5	10.2
3	-0.210	25.5	5.60	3.30	7.40	7.20	13.0	10.5
5	-0.215	25.5	5.20	2.20	7.00	5.80	12.2	8.00
7	-0.232	25.5	4.00	2.40	6.60	6.20	10.6	8.60
10	-0.247	25.5	4.20	1.60	7.60	4.70	11.8	6.30
13	-0.247	25.5	3.20	2.70	5.90	6.40	9.10	9.10
15	-0.215	25.5	2.70	2.50	5.80	6.60	8.50	9.10
23	-0.237	25.5	3.00	4.00	6.30	7.00	9.30	11.0
26	-0.218	25.5	2.30	1.00	5.50	2.70	7.80	3.70
29	-0.248	25.4	1.90	1.90	4.90	5.50	6.80	7.40
31	-0.240	25.5	1.80	1.80	4.90	5.50	6.70	7.30

TABLE 11.- NONSTEADY-STATE EXPERIMENT (NO. 11); $\alpha\beta$ MEMBRANE $\equiv$ GELMAN

GA-9, $\beta\gamma$ MEMBRANE $\equiv$ GELMAN GA-9, $c_{Na^+}^{\gamma} = 141$, $c_{K^+}^{\gamma} = 153$,

$$c_{Cl^-}^{\gamma} = 294$$

t	F_w	Temp.	c_{Na^+}	c_{Na^+}	c_{K^+}	c_{K^+}	c_{Cl^-}	c_{Cl^-}
Hours	ml/min	°C	mM	mM	mM	mM	mM	mM
0.25	-0.201	--	5.00	57.8	7.20	62.4	12.2	120
3	-0.165	28.0	12.1	9.50	15.9	15.6	28.0	25.1
4	-0.168	28.0	11.0	7.40	15.7	13.5	26.7	20.9
6	-0.172	28.0	9.60	5.20	14.2	11.3	23.8	16.5
8	-0.183	28.0	8.10	4.20	12.7	9.90	20.8	14.1
10	-0.183	28.0	7.30	3.70	11.4	9.60	18.7	13.3
13	-0.183	28.0	6.40	3.30	10.1	8.80	16.5	12.1
16	-0.184	28.0	5.50	5.70	10.9	15.9	16.4	21.6
25	-0.184	28.0	8.00	6.50	14.8	17.4	22.8	23.9
28	-0.184	28.0	6.20	7.20	14.1	15.7	20.3	22.9
31	-0.184	28.0	6.30	6.80	14.4	15.3	20.7	22.1
33	-0.184	28.0	6.30	6.30	14.6	16.2	20.9	22.5
48	-0.184	27.8	6.50	6.90	15.8	15.5	22.3	22.4

TABLE 12.- LIST OF EXPERIMENTAL CONCENTRATION AND TIME VALUES FROM

WHICH STEADY-STATE TRANSPORT RATES WERE CALCULATED

Exp. No.	$C_{Na^+}^{\alpha in}$	$C_{Na^+}^{\alpha out}$	$C_{K^+}^{\alpha in}$	$C_{K^+}^{\alpha out}$	Time for 10 ml sample
	mM	mM	mM	mM	minutes
1	85.0	87.0	85.0	87.3	51.3
2	100	90.4	100	90.4	53.8
3	100	91.0	100	88.0	33.4
4	100	89.9	100	87.5	26.8
5	100	90.3	100	87.5	25.9
6	100	90.2	100	87.5	26.0
7	100	90.0	100	87.2	27.0
8	100	90.0	100	87.2	27.3
9	40.0	45.4	40.0	47.5	41.5
10	49.0	45.3	50.8	46.8	71.1
11	50.0	45.6	50.7	45.0	36.2
12	50.0	44.0	50.5	42.0	40.1
13	50.0	44.5	50.0	43.2	28.5
14	50.0	45.0	50.0	43.3	28.3
15	50.0	45.0	50.0	43.1	29.1
16	50.0	45.0	50.0	43.0	29.5
17	14.5	22.5	13.8	24.2	37.8
18	25.0	23.4	25.0	24.5	62.7
19	25.0	20.1	25.0	19.6	71.7
20	25.0	21.2	25.0	20.3	59.3
21	25.0	21.5	25.0	20.6	60.1
22	10.0	7.95	10.0	7.25	63.0
23	4.95	4.00	5.00	3.85	64.0
24	100	87.7	100	86.8	50.5
25	100	88.0	100	85.0	39.1
26	120	96.0	120	96.9	28.9
27	140	91.0	140	91.0	33.6
28	140	92.8	140	91.0	31.0
29	140	92.2	140	91.2	22.5

APPENDIX C

Calculations

All theoretical calculations were performed by computer analysis, and the data were plotted directly from the computer printouts.

Calculations of transport rates were calculated from experimental data presented in Table 12 as follows:

$$
50) \quad \Delta J_i^{\alpha} = J_i^{\alpha out} - J_i^{\alpha in}
$$
$$
= (C_i F_{saline})^{\alpha out} - (C_i F_{saline})^{\alpha in}.
$$

For the experiments in which F_w^{α}, the water flow across the $\alpha\beta$ membrane, is zero, the flow of solution into α was equal to flow of solution out of α. This flow was determined by timing a 10 ml sample. Thus

$$
51) \quad \Delta J_i^{\alpha} = (C_i^{\alpha out} - C_i^{\alpha in}) \frac{0.01 \ L}{t \ hours} 1000
$$

where 1000 is the dilution factor.

A sample calculation of transport rate (steady-state experiment No. 5) is given below:

$$
1000 \ C_{Na^+}^{\alpha out} = 90.3 \ mM
$$
$$
1000 \ C_{Na^+}^{\alpha in} = 100 \ mM
$$
$$
t = 25.9 \ min \times \frac{1}{60} \frac{hrs}{min} = 0.432 \ hr
$$

$$
\Delta J_{Na^+}^{\alpha} = (90.3 - 100) \times \frac{0.01}{0.432} = -0.225 \ mM/hr
$$

For the experiments in which F_w^α was not zero, the saline solution flow into and out of α were different. The saline flow out of α was again determined by timing a 10 ml sample while the saline flow into α was read directly from a flow meter. The transport is now calculated as follows:

52)
$$\Delta J_i^\alpha = \left[\left(C_i^{\alpha out} \frac{0.01}{t} \right) - (C_i F_{saline})^{\alpha in} \right] 1000$$

A sample calculation of transport rate for $F_w^\alpha = 0.15$ ml/min, $F_w^\gamma = -0.437$ ml/min (steady-state experiment No. 29) is given below:

$$1000 \, C_{Na^+}^{\alpha out} = 92.2 \quad t = 22.5 \text{ min} \times \frac{1}{60} \frac{hrs}{min} = 0.375 \text{ hr}$$

$$1000 \, C_{Na^+}^{\alpha in} = 140 \quad F_{saline}^{\alpha in} = 0.294 \text{ ml/min} \times 60 \times 0.001$$
$$= 0.0177 \text{ L/hr}$$

$$\Delta J_{Na^+}^\alpha = \left[92.2 \times \frac{0.01}{0.375} - 140 \times 0.0177 \right]$$

$$= -0.013 \text{ mM/hr}$$

APPENDIX D

Analytical Manipulations

Derivation of equation 23 from 22 (19).

We define the most abundant component as the solvent, w, and write

53) $$\emptyset = \sum_{i=1}^{n}{}' J_i \cdot \text{grad} \,(-\mu_i) + J_w \cdot \text{grad} \,(-\mu_w)$$

The chemical potential, μ_i, is both pressure and concentration dependent:

54) $$\text{grad} \,(-\mu_i) = \overline{V}_i \cdot \text{grad} \,(-P) + \text{grad} \,(-\mu_i^c)$$

$\overline{V}_i$ is the partial molar volume of component i, P is the pressure at plane 0, and μ_i^c is the concentration dependent part of the chemical potential at plane 0. Similarly, for the solvent:

55) $$\text{grad} \,(-\mu_w) = \overline{V}_w \cdot \text{grad} \,(-P) + \text{grad} \,(-\mu_w^c)$$

Substituting equations 54 and 55 into equation 53 and dropping vector notations since we are considering the one-dimensional case, we have:

56) $$\emptyset = \sum_{i=1}^{n}{}' J_i\left[\overline{V}_i \text{ grad} \,(-P) + \text{grad} \,(-\mu_i^c)\right] + J_w\left[\overline{V}_w \text{ grad} \,(-P)\right.$$

$$\left. \text{grad} \,(-\mu_w^c)\right]$$

The forces grad $(-\mu_i^c)$ are not independent but are related by the Gibbs-Duhem equation which requires that

$$57) \qquad \sum_{i=1}^{n+1} C_i \text{ grad } (-\mu_i^c) = 0$$

C_i is the concentration of component i at plane 0.

Equation 57 is good for all pressures in the system. Rewriting equation 57, so as to differentiate between solvent, w, and solutes, i, we have:

$$58) \qquad \text{grad } (-\mu_w^c) = -\frac{1}{C_w} \sum_{i=1}^{n} C_i \text{ grad } (-\mu_i^c)$$

Substituting equation 58 into equation 56

$$59) \qquad = \left[\sum_{i=1}^{n} \overline{V}_i J_i + \overline{V}_w J_w \right] \text{grad } (-P) + \left[\sum_{i=1}^{n} J_i \right.$$
$$\left. \sum_{=1}^{n} \frac{C_i}{C_w} J_w \right] \text{grad } (-\mu_i^c)$$

Now, rewriting equation 59

$$60) \qquad \phi = \left[\sum_{i=1}^{n} \overline{V}_i J_i + \overline{V}_w J_w \right] \text{grad } (-P) + \sum_{i=1}^{n} \left[J_i - \frac{C_i}{C_w} J_w \right] \text{grad } (-\mu_i^c)$$

The quantity in the first bracket in equation 60 is the volume flow through the barrier:

$$61) \qquad \Gamma_V = \sum_{i=1}^{n} \overline{V}_i J_i + \overline{V}_w J_w$$

The quantity in the second bracket in equation 60 is the diffusion flow of component i relative to the solvent:

$$J_i^d = C_i(v_i - v_w)$$

$$62) \qquad J_i^d = C_i\left(\frac{J_i}{C_i} - \frac{J_w}{C_w}\right)$$

$$J_i^d = J_i - \frac{C_i}{C_w} J_w$$

v_i is the velocity of component i at plane 0 relative to a reference coordinate fixed at plane 0. Similarly, v_w is the velocity of the solvent at plane 0. Equation 60 may now be written in terms of volume and diffusion flows:

$$63) \qquad \phi = J_V \text{ grad } (-P) + \sum_{i=1}^{n} J_i^d \text{ grad } (-\mu_i^c)$$

2. Derivation of equation 29 from 26

We utilize the chain rule relating the chemical potential gradients to concentration gradients:

$$64 \qquad \text{grad } (-\mu_k^c) = \sum_{k'=1}^{n} \frac{\partial \mu_k^c}{\partial C_{k'}} \text{ grad } (-C_{k'})$$

k' is simply a new subscript for the n solutes. Substituting equation 64 into equation 26, we have

65)
$$J_i^d = \sum_{k=1}^{n} \sum_{k'=1}^{n} L_{ik}^o \frac{\partial \mu_k^c}{\partial C_{k'}} \text{ grad } (-C_{k'})$$

where (19.)

66)
$$\sum_{k=1}^{n}{'} L_{ik}^o \frac{\partial \mu_k^c}{\partial C_{k'}} = D_{ik'}$$

Equation 65 may now be written in terms of diffusion coefficients. Since k and k' have been chosen arbitrarily, they may be used interchangeably:

67)
$$J_i^d = \sum_{k=1}^{n} D_{ik} \text{ grad } (-C_k)$$

3. Demonstration of validity of neglecting cross-coupling coefficients in equation 36.

For the condition $J_i = 0$, equation 35 defines a system of differential equations:

68)
$$D_{11} \frac{dC_1}{dx} + D_{12} \frac{dC_2}{dx} - \frac{F_w}{A} C_1 = 0$$

$$D_{21} \frac{dC_1}{dx} + D_{22} \frac{dC_2}{dx} - \frac{F_w}{A} C_2 = 0$$

Let us assume solutions of the type

69) $$C_i = K_{ij}e^{\lambda_j x}$$

Substituting the solution into the system of equations we have the matrix

70) $$\begin{vmatrix} \dfrac{F_w}{A} - D_{11}\lambda_j & D_{12}\lambda_j \\ \\ D_{21}\lambda_j & \dfrac{F_w}{A} - D_{22}\lambda_j \end{vmatrix} \begin{Bmatrix} K_{1j} \\ \\ K_{2j} \end{Bmatrix} = 0$$

The characteristic equation defined by setting the determinant in the matrix equal to zero is as follows:

71) $$(D_{11}D_{22} - D_{12}D_{21})\lambda_j^2 - \dfrac{F_w}{A}(D_{11} + D_{22})\lambda_j + \left(\dfrac{F_w}{A}\right)^2 = 0$$

$D_{12}D_{21}$ in equation 71 are negligible relative to $D_{11}D_{22}$. The eigenvalues now become

72) $$\lambda_{1,2} = \dfrac{F_w}{AD_{11}}, \dfrac{F_w}{AD_{22}}$$

Neglecting the cross coefficients makes equations 68 necessarily independent, and solutions are thus

73) $$C_1 = K_1 e^{F_w x/AD_{11}}$$
$$C_2 = K_2 e^{F_w x/AD_{22}}$$

APPENDIX E

Error Analysis

1. Flow readings

The manufacturer of the flow meters employed in this study gave the expected error of the flow readings to be 2% of the full scale reading of 0.5 ml/min for a sapphire float and 1.0 ml/min for a stainless steel float. This was consistent with observations made during calibration of the flowmeters.

2. Determinations of Na^+ and K^+ concentrations in compartment β and γ:

Procedure		Error
a.	0.1 ml sample by syringe:	±0.001 ml
b.	Addition of 5 ml water (min. dilution):	±0.04 ml
c.	Sample into 100 ml volumetric flask (max. dilution):	±0.08 ml
d.	Concentration determination by atomic absorption spectrophotometry:	±0.001 mM
e.	Estimated maximum error:	±5%

3. Determinations of Na^+ and K^+ transport, ΔJ_i^α, $F_w^\alpha = 0$

a.	Collection of 10 ml sample:	±0.02 ml
b.	Timing of the collection:	±0.1 min
c.	Pipetting of 1.0 ml from the 10 ml sample:	±0.01 ml
d.	Dilution of 1.0 ml in 1.0 L volumetric flask:	±0.3 ml
e.	Concentration determination by atomic absorption spectrophotometry:	±0.001 mM
f.	Estimated maximum error:	±22%

APPENDIX F

List of Symbols

A	total membrane pore area
$A^{\alpha\beta}$	total membrane pore area of $\alpha\beta$ membrane
$A^{\beta\gamma}$	total membrane pore area of $\beta\gamma$ membrane
$b_{ik}^{\alpha\beta}$	coefficient equal to $\left(\dfrac{AD_{ik}^*}{\Delta X}\right)^{\alpha\beta}$
$b_{ik}^{\beta\gamma}$	coefficient equal to $\left(\dfrac{AD_{ik}^*}{\Delta X}\right)^{\beta\gamma}$
C_i	concentration of component i
$C_i^{\alpha}, C_i^{\beta}, C_i^{\gamma}$	concentration of component i in compartment α, β, and γ, respectively
C_w	concentration of water in solution
D_{ik}	diffusion coefficient relating the ith flow to the kth force
D_{ik}^*	average diffusion coefficient over integrated values
D_{11}	diffusion coefficient relating the flow of Na^+ to the Na^+ concentration gradient
D_{12}	diffusion coefficient relating the flow of Na^+ to the K^+ concentration gradient
D_{21}	diffusion coefficient relating the flow of K^+ to the Na^+ concentration gradient
D_{22}	diffusion coefficient relating the flow of K^+ to the K^+ concentration gradient
E	electrical potential

e	exponential
F	Faraday constant
F_w^{α}	flow of water across $\alpha\beta$ membrane
F_w^{γ}	flow of water across the $\beta\gamma$ membrane
$F_{saline}^{\alpha in}$	flow of solution into compartment α
$F_{saline}^{\alpha out}$	flow of solution out of compartment α
f_{ik}	frictional coefficient between components i and k
J_i	flow of component i
$J_i^{\alpha\beta}$	flow of component i across the $\alpha\beta$ membrane
$J_i^{\alpha\beta}$	flow of component i across the $\beta\gamma$ membrane
$J_i^{\alpha in}$	flow of component i into compartment α
$J_i^{\alpha out}$	flow of component i out of compartment α
J_i^d	flow of component i relative to the flow of solvent
J_D	diffusion flow
J_V	volume flow
J_w	flow of water
k_o, k_o, k_{ij}	eigenvector
L_{ik}	phenomenological coefficient relating the ith flow to the kth force
L_p	mechanical filtration coefficient for membrane
L_p^o	mechanical filtration coefficient for differential thickness of membrane
L_{PD_k}	phenomenological coefficient relating volume flow to the chemical potential gradient of the kth component

L_{DP_i} phenomenological coefficient relating diffusion flow of component i to pressure gradient

$M_{1,2}, M_{2,1}$ unidirectional material fluxes from one side of membrane to the other

M   summation of membrane parameters and frictional coefficients

n   total number of solutes

$n_i^\alpha, n_i^\beta, n_i^\gamma$ total moles of component i in compartments α, β, and γ

$\dot{n}_i$ transport rate

$\dot{n}_L$ lactic acid production

O   reference plane within membrane

P   pressure

Q   heat

q_j production or consumption rate of component i

R   universal gas constant

R_{ik} resistance coefficient relating the ith force to the kth flow

S   entropy

T   absolute temperature

t   time

V   volume

$V^\alpha, V^\beta, V^\gamma$ volumes of compartments α, β, and γ

$\bar{V}_k$ partial molar volume of component k

v_i velocity of component i

v_w velocity of water

w   water

X_i ith force

x direction

Δx boundary thickness

dx differential boundary thickness

z ion valence

α compartment analogous to the kidney tubule lumen

β compartment analogous to tubule cell volume

γ compartment analogous to interstitial fluid compartment

γ_k activity coefficient of component k

$\eta^{\alpha\beta}, \eta^{\beta\gamma}$ empirical parameter representing apparent ratio of membrane

         pore area to boundary thickness to the ratio of membrane

         pore area to membrane thickness as given by the membrane

         manufacturer for the $\alpha\beta$ and $\beta\gamma$ membranes

θ empirical parameter representing ratio of apparent water

         velocities to experiment water flux

λ_j eigenvector

μ_i chemical potential of component i

μ_i^c concentration dependent part of chemical potential of

         component i

σ local entropy production

σ reflection coefficient

ϕ dissipation function

ω mobility

ABSTRACT

OF

A NONEQUILIBRIUM THERMODYNAMIC

MODEL OF ION TRANSPORT IN A THREE-COMPARTMENT SYSTEM

By

Heinz George Hausch
Department of Physiology
Medical College of Virginia

A physical analog of steady-state sodium and potassium transport

in a two-membrane, three-compartment system was studied utilizing the

principles of nonequilibrium thermodynamics. This physical system is

analogous to physiological systems where one compartment consisting of

a cell monolayer separates two other compartments, such as the inter-

stitial fluid and the renal tubule lumen in the kidney. The membranes

in the model system serve only to localize the chemical potential

gradients between compartments. The phenomenological equations relating

the flows through the membranes to the chemical potential gradients

were developed from the equation for energy dissipation within each

membrane. The flows defined both the nonsteady-state rates of change

of concentrations within each compartment and the steady-state transport

across each membrane.

Ion transport due to chemical convection was studied by adding

water to the "cell" compartment and removing it from the "interstitial"

compartment. The "lumen" compartment was left as a strictly passive

compartment. The Na^+, K^+, and Cl^- concentrations were measured

periodically until a steady-state was reached.

In further experiments the concentrations of components in the "lumen" compartment were held constant by a constant flow of $NaCl-KCl-H_2O$ solution through the compartment. The constant flow of water into the "cell" compartment distributed itself among both the "lumen" and "interstitial" compartments according to the mechanical filtration properties of each membrane. In initial experiments, the flows were unidirectional into the "interstitial" compartment. In later experiments the flow was distributed to both the "interstitial" and "lumen" compartment. After the system had reached a steady-state, the concentration of components, the flows in and out of the "lumen" compartment and the flow of water into the "cell" compartment were measured. The magnitudes and directions of the steady-state transport of components were determined.

The nonsteady-state experiments demonstrated a transient transport of Na^+, K^+, and Cl^- ions from the "lumen" compartment to the "interstitial" compartment against a concentration gradient. At low solvent fluxes the ion transport occurs with the concentration gradient. At intermediate solvent fluxes, K^+ and Na^+ are transported in opposite directions; K^+ is transported down a concentration gradient while Na^+ is transported against an equal or larger gradient.

Steady-state transport of Na^+ and K^+ from the "lumen" compartment to the "interstitial" compartment may be maintained by a solvent flux in the direction of transport. The magnitude of this transport is greatest when the concentrations of components in the two compartments

are equal, and decreases as the concentration ratio of components in the "intestitial" compartment to those in the "lumen" increases. For the combinations of solvent fluxes and component concentrations investigated, the transport of K^+ was usually greater than the transport of Na^+.